Vulnerability Model for Cantilever Retaining Walls Subject to Scour

Lanting Wei[1], Alessandro Tarantino[2], Enrico Tubaldi[3*], Hamed Moghaddasi[4], and Daniele Zonta[5]

[1]Dept. of Civil and Environmental Engineering, Univ. of Strathclyde, Glasgow, UK; [2]Dept. of Civil and Environmental Engineering, Univ. of Strathclyde, Glasgow, UK; [3]Dept. of Civil and Environmental Engineering, Univ. of Strathclyde, Glasgow, UK; Email: enrico.tubaldi@strath.ac.uk; [4]Dept. of Civil and Environmental Engineering, Univ. of Strathclyde., Glasgow, UK;[5]Dept. of Civil, Environmental and Mechanical Engineering, Univ. of Trento, Via Mesiano, Trento, Italy*

For Peer Review

Vulnerability Model for Cantilever Retaining Walls Subject to Scour

Abstract: Retaining walls are widely used to stabilize slopes and support infrastructure such as bridge abutments, culverts, and roads over or adjacent to waterways. These structures can be susceptible to scour-induced erosion and undermining at their toe, which can lead to significant damage and collapse. This paper presents a comprehensive yet simplified analytical formulation to evaluate the reduction in retaining wall capacity caused by scour. First, a model is proposed to describe the scour process at retaining walls. Based on this model, the degradation of retaining wall capacity is formulated by considering various potential failure modes. The proposed formulation, validated against numerical simulations using PLAXIS, is non-dimensionalised to derive simple expressions for describing the effect of scour across different wall geometries, soil properties, and water depths. A simplified approach is then introduced to estimate the scour vulnerability of retaining walls, expressing the conditional probability of wall failure with increasing scour levels. The study provides a practical tool for engineers and infrastructure asset managers to support rapid risk prioritization of retaining walls exposed to scour, highlighting the most critical parameters influencing the vulnerability of these structures.

Keywords: Scour; Vulnerability; Retaining walls; Closed-form solution; Flooding.

1.Introduction

Retaining walls are commonly employed to stabilize slopes and support transport infrastructure elements such as bridge abutments, culverts, and over or adjacent to waterways. These structures are susceptible to scour-induced erosion and toe undermining, which can lead to significant damage and structural failure (Khosronejad, Diplas et al. 2020). Scour at the base of retaining walls is typically associated with four mechanisms: (i) general scour, resulting from the natural evolution of waterways that lowers the elevation of river channels; (ii) constriction scour, where a reduction in river width increases flow velocity within the channel; (iii) local scour, which occurs at the leading edge of retaining walls due to high-energy turbulence; and (iv) bend scour, which affects retaining walls along outer banks of meandering rivers due to sudden changes in flow velocity and direction at bends. The

For Peer Review

interaction of these scour mechanisms can significantly increase the risk of retaining wall failure (Heydari and Diplas 2020). This risk can also be significantly exacerbated by the ageing of these structures and the intensification of extreme weather events and floods due to climate change.

While the vulnerability of bridges to scour has been extensively investigated (Argyroudis and Mitoulis 2021, Tubaldi, White et al. 2022, Scozzese, Tubaldi et al. 2023), research on the vulnerability of retaining walls remains limited. Guidelines and standards on scour risk assessment, such as CIRA manuals SP171 and C742 (CIRIA 2015, CIRIA 2021), CS 469 (NationalHighways 2024) and French guidelines (Cerema 2019) provide limited information on the evaluation of the scour risk of retaining walls. Furthermore, scour is frequently overlooked in the design of retaining walls located adjacent to watercourses, a practice that has been associated with catastrophic failures (McKelvey, 2011). Thus, there is a need to develop scour vulnerability and risk assessment procedures accounting for the specific features of these structures.

The hydraulic processes responsible for scour at the base of longitudinal training walls differ from those acting on bridge piers. A key distinction is that, along retaining walls, lateral flow typically generates elongated scour patterns, whereas pier scour is dominated by downflow and the formation of a horseshoe vortex at the upstream face. Some studies have examined the hydraulic aspects of the problem, especially the evaluation of the scour depth along walls (Heydari and Diplas 2020). Different approaches have been proposed for estimating the scour depth in longitudinal structures through experimental flume studies and empirical formulations (Fael, Simarro-Grande et al. 2006, Khosronejad, Diplas et al. 2020, Calixto, Castaño et al. 2023, Sotiropoulos and Diplas 2017). It has been found that the development of a scour hole is influenced by a wide range of hydraulic, geotechnical factors and geometry of

For Peer Review

the problem, including the wall's orientation relative to the approaching flow, local flow velocity and turbulence intensity, sediment transport capacity, and the properties of the riverbed material (Calixto, Castaño et al. 2023, Sotiropoulos and Diplas 2017). Other studies, discussed in Huang (2017), have investigated the failure mechanisms for reinforced retaining walls under toe scouring action, with primary emphasis on coastal settings. However, despite the efforts made on understanding the hydraulic processes and evaluating the scour depth along retaining walls, the influence of scour on the stability of retaining walls has not received sufficient attention. To the best of the author's knowledge, no previous studies have explicitly proposed models to describe the scour vulnerability of these structures.

The evaluation of the impact of scour on the capacity of retaining walls is a complex task, which must consider the likelihood of occurrence of several failure modes, namely the exceedance of the foundation bearing capacity, the sliding at the base of the foundation, and the structure overturning (Theinat et al., 2024). The geometry of the walls, the properties (e.g. friction angle and cohesion) of the backfill and base soil, as well as the water level, all play an important role in the vulnerability assessment and affect both the demand and the capacity. Although advanced numerical models can be developed for investigating the vulnerability of retaining walls, there is a need for vulnerability models which are simple enough to be embedded in standards and used for identifying those walls that are more vulnerable to scour.

This study illustrates a simple yet accurate analytical formulation for evaluating the effect of scour on the safety factor of retaining walls. The proposed formulation uses Lancellotta's earth pressure coefficients to calculate active and passive thrusts (Lancellotta 2002) accounting for wall friction and the bearing capacity model of Hansen and Vesić (Hansen 1970, Vesić 1973), with both models further extended to consider the effect of scour. Validated against the results of advanced numerical analysis of retaining walls in PLAXIS

For Peer Review

(PLAXIS 2020), the proposed formulation accounts for the various possible limit states that could result in wall failure due to scour.

The analytical formulation is non-dimensionalised, and global sensitivity analysis is performed with the aim of deriving a simple curve that describes the reduction in the partial safety factor with increasing scour levels, accounting for wall geometry, soil properties, and water height. The proposed curve can be used for the preliminary assessment of retaining walls and the identification of the most critical parameters that control the wall's safety. In the last part of the paper, fragility functions are developed to describe the conditional probability of wall failure with increasing scour levels.

The rest of the paper is organised as follows. A description of the various actions, resisting mechanisms and limit state functions that underpin the proposed closed-form formulation for the evaluation of the impact of scour on the safety of retaining walls is provided first. Following this, the validation of the formulation is presented, using advanced numerical models developed in PLAXIS (PLAXIS 2020) for three case studies. Next, the paper introduces the non-dimensional formulation that describes the reduction in safety of retaining walls with increasing levels of normalised scour depth, along with the results from global sensitivity analyses that highlight the influence of model parameters on the non-dimensional outcomes. The development of simplified fragility functions for retaining walls exposed to scour is then presented, followed by a conclusion section.

2. Actions and resisting mechanisms for retaining walls exposed to scour

2.1 Problem geometry

Figure 1 illustrates the geometry of the idealised model used to represent both cantilever and gravity retaining walls.

For Peer Review

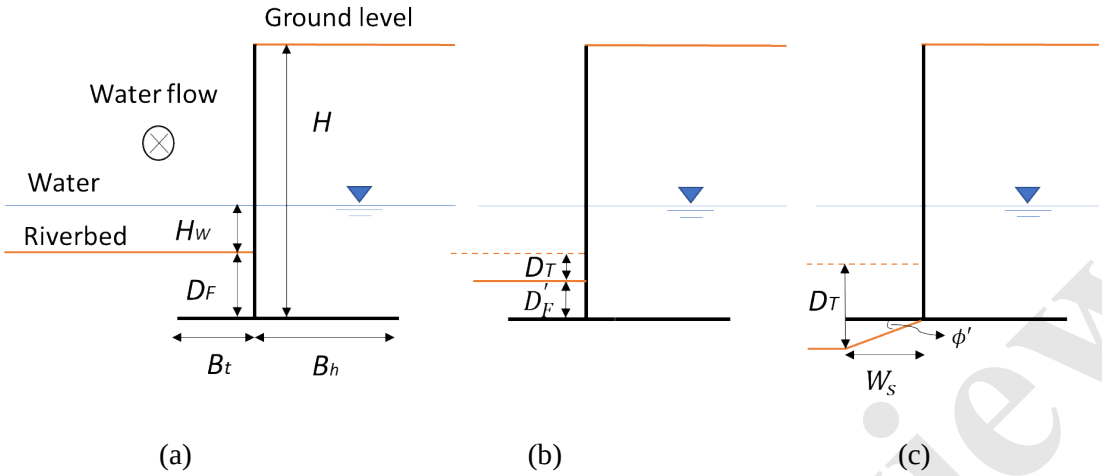

Figure 1 Idealised model of retaining wall: (a) case of no scour (b) scour in stage 1: $D_T \leq D_F$ (c) scour in stage 2: $D_T > D_F$

The wall has a total height H, and a foundation width of B, which is made up of the toe length B_t and the heel length B_h. The wall is embedded into the riverbed, with D_F representing the depth from the riverbed surface to the base of the foundation. The water height H_w refers to the vertical distance from the riverbed to the water surface.

Scour is assumed to progress in two stages: first, the riverbed soil is eroded uniformly (Figure 1b) until the base of the foundation is reached and the toe is fully exposed. Then, the soil at the base of the foundation is undermined, from the edge of the toe towards the heel, as illustrated in Figure 1c. The maximum depth of scour below the riverbed is denoted as D_T. During the first stage (i.e., $D_T \leq D_F$ in Figure 1b), increasing levels of scour correspond to a reduction of the embedded depth:

$$D'_F = \max(0, D_F - D_T) \quad (1)$$

For Peer Review

During the second stage (i.e, D_T>D_F in Figure 1c), scour undermines the bottom of the foundation and progresses horizontally from the toe to the heel, with a width W_s defined by Equation (2).

$$W_s = \frac{D_T - D_F}{tan\phi'} \quad (2)$$

where the angle of inclination of the scour hole is assumed equal to the effective soil friction angle ϕ'. This assumption idealizes the scour slope as being controlled only by riverbed material properties. In reality, scour slope angles are also influenced by other factors including wall angles relative to the approach flow, flow velocity and turbulence, sediment transport capacity, and time dependent scour development etc. (Calixto, Castaño et al. 2023, Sotiropoulos and Diplas 2017). The adopted scour angle is therefore intended as a simplified representation for modelling purposes and should be interpreted within the limitations of this assumption.

Figure 2 illustrates actions and resisting mechanisms for retaining walls exposed to scour. The wall is subjected to the active thrust S_a at the edge of the heel and the passive thrust S_p at the edge of the toe. The soil exerts a gravity force W_h and W_t on the heel and toe, respectively. As a result of these actions, the base is subject to a total vertical force N and a total horizontal force T. The total vertical force N is applied with an eccentricity e, measured from the centre of the effective foundation width B'- the portion of the base still in contact with the soil after scour. The maximum horizontal force T_{lim} and the maximum vertical force Q_{lim}, acting beneath the wall base, represent the thresholds beyond which sliding and bearing capacity failures are initiated, respectively.

For Peer Review

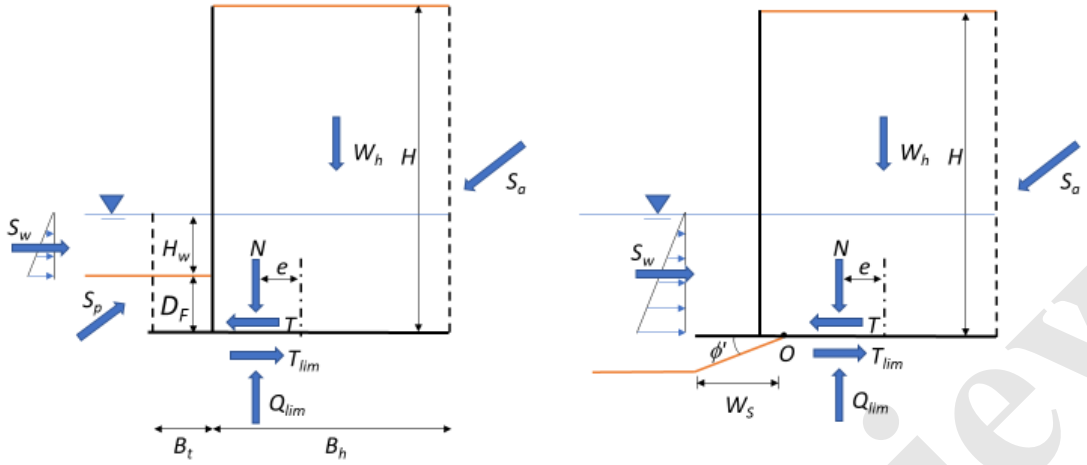

(a) (b)

Figure 2. Sketch of a cantilever wall for the case of (a) no scour (b) scour undermining the foundation.

Failure of retaining walls can occur through three mechanisms. Bearing capacity failure occurs when the applied normal force N exceeds the limiting capacity $Q_{lim.}$ Sliding failure takes place when the driving shear force T surpasses the available resistance T_{lim}. Overturning failure happens when the destabilizing moment exceeds the stabilizing moment, with both these moments measured with respect to the point of intersection between the scour hole and the foundation base (i.e., point O in Figure 2b).

2.2 Active and passive thrusts

Accurate estimation of the active thrust S_a and passive thrust S_p is crucial for assessing the stability of retaining walls under all failure mechanisms. The earth pressures should also account for the impact of water. On the backfill side, water adds horizontal hydrostatic force to the active earth pressure on the lower portion of the wall. On the riverside, with water above the riverbed, the weight of water increases the passive pressure. The earth pressures are also affected by scour. With wall friction considered, scour changes the vertical component

For Peer Review

of passive pressure, therefore influencing sliding resistance, overturning moments, and the overall geotechnical demand.

The active thrust S_a is given in Equations (3)-(5) and the passive thrust S_p is in Equations (6)-(8); their expressions are based on the coefficient k_a for active thrust and k_p for passive thrust derived using the lower bound theorem of plasticity (Lancellotta 2002). Each earth pressure consists of two parts, with a different pressure distribution and point of application, requiring separate consideration during moment equilibrium calculations for accurate stability assessment. For active pressure, $S_{ah,1}$ is the active pressure from the retained soil, whereas $S_{ah,2}$ accounts for hydrostatic water pressure, which acts partially on the lower portion of the soil-wall system. For passive pressure, $S_{ph,1}$ is the passive pressure, and $S_{ph,2}$ represents the weight of overlying water forming a rectangular pressure distribution. Both passive pressure components change with scour. Due to friction at soil-wall interface, the effective vertical component of earth pressure forms an angle δ with the effective horizontal component, where δ is assumed equal to soil friction angle ϕ'. It should be noted that the soil–wall interface is actually a soil–soil interface, since the soil above the heel is treated as an integral part of the retaining wall. The development of the expressions for earth pressures is illustrated in Appendix 1.

$$S_{ah} = \underbrace{\frac{1}{2} k_a \gamma H^2}_{S_{ah.1}} + \underbrace{\frac{1}{2}(1 - k_a)\gamma_w (H_w + D_F)^2}_{S_{ah.2}} \tag{3}$$

$$k_a = (1 - \sin\phi')e^{-\left(\frac{\pi}{2} - \phi'\right)\tan\phi'} \tag{4}$$

$$S_{av} = \frac{1}{2}\tan\phi' \, k_a \gamma H^2 - \frac{1}{2}\tan\phi' \, k_a \gamma_w (H_w + D_F)^2 \tag{5}$$

For Peer Review

$$S_{ph} = \underbrace{\frac{1}{2}\gamma k_p D_F'^2 + \frac{1}{2}(1-k_p)\gamma_w D_F'^2}_{S_{ph,1}} + \underbrace{\gamma_w (H_w + D_F - D_F')D'_F}_{S_{ph,2}} \quad (6)$$

$$k_p = (1+\sin\phi')e^{\left(\frac{\pi}{2}+\phi'\right)\tan\phi'} \quad (7)$$

$$S_{pv} = \frac{1}{2}(\gamma - \gamma_w)k_p^* = \tan\phi'\, k_p D_F'^2 \quad (8)$$

2.3 Bearing capacity

Scour impacts the bearing capacity by reducing the embedded depth and the effective soil-foundation interface, and this in turn changes the eccentricity and the inclination of the resultant load on the riverbed. The change in eccentricity further reduces the effective width of the foundation. To capture these effects, the bearing capacity formulation is developed for the three scenarios illustrated in Figure 1. The riverbed soil is assumed to be cohesionless and homogeneous, with its effective friction angle remaining unchanged by scour.

In the absence of scour, the effective bearing capacity q'_{lim} is given by the following expression based on Hansen and Vesić's approach (Hansen 1970, Vesić 1973):

$$q'_{lim} = \frac{1}{2}\gamma B' N_\gamma i_\gamma + \gamma D_F N_q i_q \quad (9)$$

where B' is the effective foundation width, given by:

$$B' = B_h + B_t - 2e \quad (10)$$

In Equation (10), N_q and N_γ are dimensionless factors depending on the friction angle of the

For Peer Review

soil, and i_q and i_γ are surcharge inclination angles depending on the ratio between the horizontal and vertical force, *T* and *N*.

$$N_q = \frac{1+\sin\phi'}{1-\sin\phi'}\exp(\pi\tan\phi') \tag{11}$$

$$N_\gamma = 1.5\left(N_q - 1\right)\tan\phi' \tag{12}$$

$$i_q = \left(1-\frac{T}{N}\right)^2 \tag{13}$$

$$i_\gamma = \left(1-\frac{T}{N}\right)^3 \tag{14}$$

For low scour depths such that the foundation is not undermined ($D_T \leq D_F$), q'_{lim} is given by:

$$q'_{lim} = \frac{1}{2}\gamma B' N_\gamma i_\gamma + \gamma D F' N_q i_q \tag{15}$$

When scour reaches the base of the foundation ($D_T > D_F$), undermining a portion W_s of the foundation, q'_{lim} is given by:

$$q'_{lim} = \frac{1}{2}\gamma B' N_\gamma i_\gamma \tag{16}$$

$$B' = (B_h + B_t - W_s) - 2e \tag{17}$$

A positive eccentricity *e* means the resultant force *N* is positioned to the left of the effective foundation centre. When scour occurs but the foundation is not undermined (i.e. $D_T \leq D_F$), moment equilibrium results in an eccentricity with respect to the mid-point of the effective

For Peer Review

foundation by Equation (18).

$$e = \frac{W_t \frac{B_h}{2} + S_{ah,1} \frac{H}{3} + S_{ah,2} \frac{H_w + D_F}{3}}{W_t + W_h + S_{av} - S_{pv} - U} - \frac{W_h \frac{B_t}{2} + S_{av}\left(\frac{B_h + B_t}{2}\right) + S_{ph,1} \frac{D'_F}{3} + S_{ph,2} \frac{D'_F}{2} + S_{pv}\left(\frac{B_h + B_t}{2}\right) + S_w\left(\frac{H_w + D_T}{3} + D'_F\right)}{W_t + W_h + S_{av} - S_{pv} - U} \quad (18)$$

When scour undermines the foundation (i.e., $D_T > D_F$ and $Ws > 0$), moment equilibrium introduces an eccentricity by Equation (19).

$$e = \frac{W_t \frac{B_h + W_s}{2} + S_{ah,1} \frac{H}{3} + S_{ah,2} \frac{H_w + D_F}{3} - W_h \frac{B_t - W_s}{2} - S_{av}\left(\frac{B_h + B_t - W_s}{2}\right)}{W_t + W_h + S_{av} - S_{pv} - U} + \frac{-S_w\left(\frac{H_w + D_F}{3}\right) - U\frac{W_s}{2}}{W_t + W_h + S_{av} - S_{pv} - U} \quad (19)$$

The total bearing force Q_{lim} is the sum of effective bearing force and buoyancy force, given by:

$$Q_{lim} = \left[q'_{lim} + \gamma_w (D_F + H_w)\right] B' L \quad (20)$$

2.4 Other actions and resisting mechanisms

The soil-foundation interface is subjected to resultant action forces, including a driving shear force T, which is the sum of horizontal earth pressures and horizontal water pressure, and a vertical resultant force N, which is the sum of the soil weight (adjusted for buoyancy) and vertical passive pressure. They are expressed as:

$$T = S_{ah} - S_{ph} - S_w \quad (21)$$

$$N = W_t + W_h + S_{av} - S_{pv} - U \quad (22)$$

For Peer Review

The force applied to the toe W_t consists of the weight of the soil and of the water above it, influenced by scour actions. The force on the heel W_h represents the weight of the retained soil and water, remaining unaffected by scour. These forces are expressed as follows:

$$W_t = B_t[D'_F\gamma + (H_w + D_F - D'_F)\gamma_w] \tag{23}$$

$$W_h = B_h\gamma H \tag{24}$$

where γ denotes the equivalent soil unit weight, which is the total weight of the saturated and unsaturated soil divided by the relevant overall soil volume.

The stem, i.e., the vertical structural element that directly retains the soil, is subject to the water thrust on the toe side S_w, which increases as the soil layer diminishes and the scour progresses, whose expression is:

$$S_w = \frac{1}{2}\gamma_w(H_w + D_F - D'_F)^2 \tag{25}$$

The wall-soil system is subject to the buoyancy force U, which is unaffected by scour and is given by:

$$U = (H_w + D_F)\,(B_t + B_h)\gamma_w \tag{26}$$

3. Limit-state functions

Three different limit-state functions are formulated to describe the failure mechanisms, namely geotechnical failure, overturning failure, and sliding failure. Geotechnical failure occurs if the vertical surcharge N exceeds the bearing capacity Q_{lim}, which corresponds to the bearing capacity factor f_{bc} defined below exceeding 1:

For Peer Review

$$f_{bc} = \frac{W_t + W_h + S_{av} - S_{pv}}{Q_{lim}} \quad (27)$$

Overturning failure occurs when the destabilising moments exceeding the stabilising moments, i.e. when the overturning factor defined in equation (28) exceeds 1. When the foundation is not undermined, overturning is measured at the edge of the foundation on the waterside. When scour undermines the foundation, the overturning of the retaining wall is measured at the point O of Figure 2b. As scour progresses, this point moves past the centre of the toe, foundation, and heel, and stabilizing forces become destabilizing. To account for this, various expressions of the overturning factor need to be considered; these are detailed in Appendix 2.

$$f_{ov} = \frac{M_{de}}{M_{st}} \quad (28)$$

Where M_{st} and M_{un} denote respectively the stabilising and destabilising moments.

Sliding failure occurs when driving sliding force T exceeds the sliding resistance T_{lim}, which corresponds to the sliding factor f_{sl} defined below exceeding 1.

$$f_{sl} = \frac{S_{ah} - S_{ph} - S_w}{(W_t + W_h + S_{av} - S_{pv} - U)\tan\phi'} \quad (29)$$

4. Strength reduction method

The stability of retaining walls at any given scour D_T can be evaluated using the three failure mechanisms described above, each based on its respective limit state function. The factor of safety for each of these mechanisms is assessed via the Strength Reduction Method (SRM) (EN 1997). The partial safety factor $\gamma_{\phi'}$ represents the reduction factor of the shearing

For Peer Review

resistance required to bring the soil to the onset of collapse. The factor of safety is quantified the ratio between the tangent of the actual friction angle, $\tan\phi'$, and the tangent of the friction angle associated with the onset of failure, $\tan\phi'_{crit}$.

$$\gamma_{\phi'} = \frac{\tan\phi'}{\tan\phi'_{crit}} \tag{30}$$

Let us consider the case of a retaining wall initially stable. To cause the retaining wall to fail, the $\tan\phi'$ needs to be decreased to a critical value $\tan\phi'_{crit}$ until collapse occurs. The reduction in soil friction angle affects both the demand and capacity in all failure mechanisms; it increases the active thrust and reduces the passive thrust respectively, thereby increasing the risk of sliding and overturning. At the same time, the lower friction angle underneath the foundation decreases the bearing capacity Q'_{lim} and decreases the sliding resistance T_{lim}, thus increasing the likelihood of failure by exceedance of bearing capacity and sliding.

Figure 3 shows an example of the resistance-to-action ratio for the three failure mechanisms against the reduction factor. As the reduction factor increases, soil friction angle reduces, and the resistance-to-action ratio also reduces. The intersection points between the resistance-to-action curve and the horizontal red line, where resistance-to-action equals 1, identify the partial safety factor for the individual mechanisms. The partial safety factor $\gamma_{\phi'}$ for the retaining wall is the minimum partial safety factors between the three mechanisms (the bearing capacity in the example shown in Figure 3). This corresponds to considering the system reliability as a series system, similarly to Daryani and Mohamad (2014).

For Peer Review

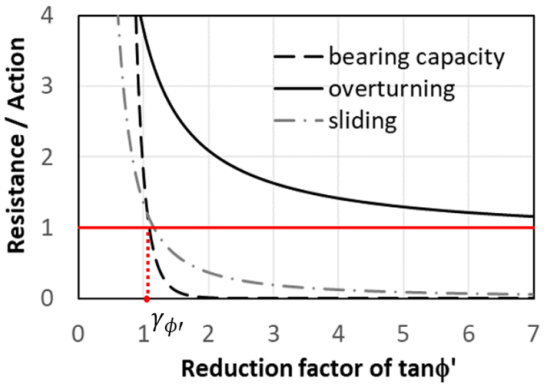

Figure 3. Resistance-to-action ratio and the reduction factor of $\tan\phi'$. Example of a retaining wall with the geometry of H=4.05 m, D_T=0, B_h=1.2 m, B_t=1.3 m, $D_F = H_w = \gamma_w = \delta = 0$, $\phi' = 28°$.

5. Model validation

The proposed closed-form solution is validated against numerical modelling using three structures representative of retaining walls in the UK road transport network. For each case study, the curve describing the reduction in the safety factor with increasing scour levels, derived from the section 2-4, is compared with the corresponding curve obtained using PLAXIS (PLAXIS 2020).

Figure 4 illustrates the transverse section of the walls and the corresponding simplified model used in the proposed formulation. The retaining wall in Figure 4a is modelled as a wall with no toe, whereas the one in Figure 4b as a wall with a toe and a heel. The retaining wall in Figure 4c is a typical cantilever wall with an inverted 'T' shape, which mostly utilize the weight of the backfill soil to provide the resistance to failure.

For Peer Review

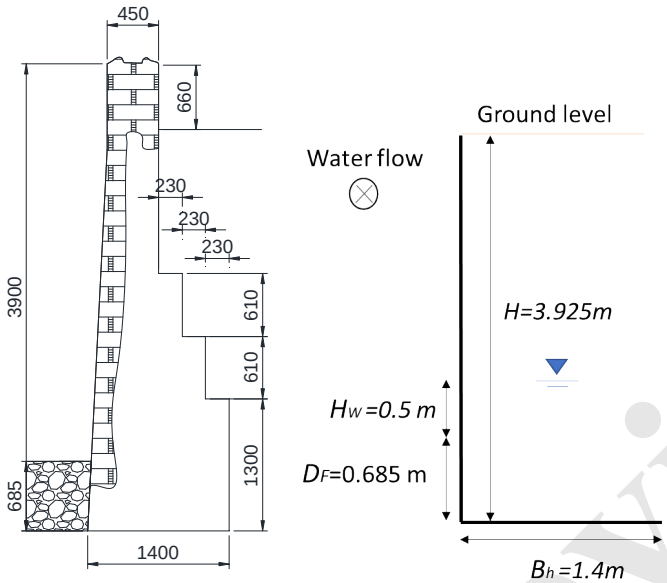

(a)

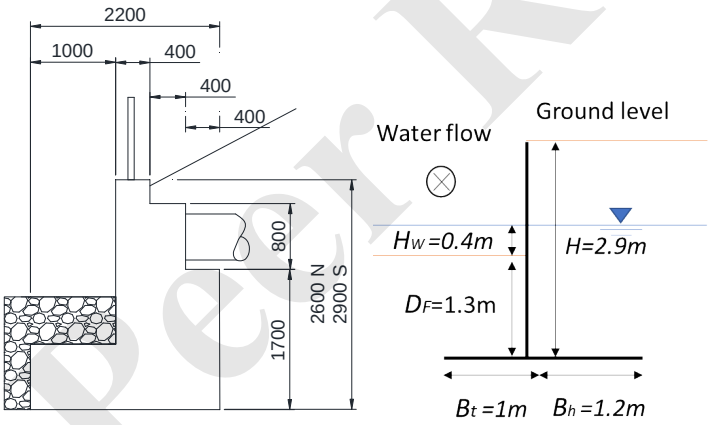

(b)

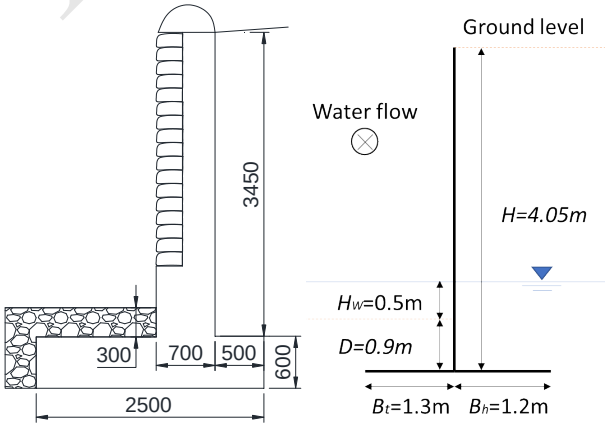

(c)

For Peer Review

Figure 4 Section drawings of retaining walls adjacent to the riverbank and their equivalent geometry in the closed-form solution. (a) retaining wall 1 (RW1) (b) retaining wall 2 (RW2) (c) retaining wall 3 (RW3)

Numerical models of the selected case studies, developed in PLAXIS 3D Version 20.03 (PLAXIS 2020), are used to calculate the variation of the factor of safety with increasing scour levels. To eliminate the impact of the boundaries on the results, the soil domain's height and width are set to be 8 times and 10 times the height of the wall, respectively. The ground has the displacement constrained in the out-of-plane direction to simulate a plane strain state. The mesh is refined into three zones, becoming progressively finer near the wall to enhance the accuracy of capturing soil deformation in its vicinity. The backfill and foundation soil are modelled with a homogeneous elasto-plastic material model with the failure surface described by the Mohr–Coulomb criterion, defined by the parameters Young's modulus $E_{ref}^{'}$ (kN/m^2), Poisson's ratio v, friction angle ϕ'(°), Dilatancy angle ψ' (°), Cohesion c' (kPa). It is noteworthy that the value of the friction angle of 20° used for the analysis of RW2 is rather low and has been considered here purely as an illustrative example, representing loose alluvial soils from riverbed material with low strength and bearing capacity. The retaining wall is represented by an elastic material with Young's moduli representing concrete with a compressive strength of 25 MPa (ACI 2011). Between the soil and the wall, interface elements are introduced. The stiffness and strength properties of the interfaces are derived from those of the surrounding soil. Table 1 illustrates the values adopted for the parameters of the three models.

Table 1. Values of parameters of PLAXIS models

Soil properties						Wall Properties		
Young's modulus $E_{ref}^{'}$ (kN/m^2)	Poisson's ratio v	Friction angle ϕ' (°)	Dilatancy angle ψ' (°)	Cohesion c' (kPa)	Bulk density γ (kN/m^3)	Young's modulus $E_{ref}^{'}$ (kN/m^2)	Poisson's ratio v	Density (kN/m^3)

For Peer Review

25700	0.286	RW1: 35 RW2: 20 RW3: 28	RW1: 35 RW2: 20 RW3: 28	0	20	23500000	0.15	25

Each case study was analysed in PLAXIS using a three-stage construction procedure. In the first stage, the retaining wall and the initial ground conditions were activated and brought to equilibrium. In the second stage, the scour process was simulated by progressively removing soil elements around the wall until a new equilibrium state was achieved. In the final stage, a strength-reduction analysis was performed, in which the shear strength parameters ϕ' and c were systematically reduced to identify the onset of global failure of the retaining wall system.

Figure 5 to Figure 7 illustrate the contour plot of the incremental deviatoric strains ε_q at the final step of the analysis for the selected case studies, under conditions of no scour and varying scour levels. The patterns of incremental deviatoric strains are similar at point A (no scour) and point B (scour depth equal to embedment depth). In both situations, failure planes develop across the backfill soil and extend below the foundation and towards the riverbed. When the foundation is undermined by scour (point C), the failure surfaces are still located below the foundation and within the backfill soil, but the affected area is smaller than in previous stages, suggesting a localisation of deformations. As scour progresses further (point D), the deviatoric strains are concentrated primarily near the back of the wall, suggesting that the overturning mode becomes critical when the critical scour condition is approached.

Figure 5 to Figure 7 also show the curves describing the reduction of safety factor based on the closed-form solutions for sliding, overturning, and foundation bearing capacity limit state, and the curve derived from the numerical analysis. For $D_T < D_F$, the sliding failure is the critical failure mechanism in RW2 and RW3. However, as scour progresses ($D_T \geq D_F$), the

For Peer Review

foundation bearing capacity limit state is characterised by the lowest safety factor and controls the failure. It is also worth observing that the curves for the overturning and bearing capacity limit state tend to converge to the same point at zero capacity. According to the proposed formulation, this point corresponds to the location of the resultant of the vertical loads. If the horizontal penetration of scour progresses beyond this point, equilibrium is not possible. This observation has important implications for the definition of a simplified expression for the reduction of safety of retaining walls due to scour in Section 2-4.

In general, it is interesting to observe that for low levels of scour, the safety factor reduces almost linearly for increasing scour levels, whereas for high levels of scour, a nonlinear, more significant reduction is observed until the critical condition of zero capacity is attained. Despite its underlying simplifying assumptions, the proposed formulation provides results quite close to the numerical results. The discrepancy between the results can be attributed mainly to the assumption of independent failure mechanisms and the fact that the bearing capacity is calculated using a semi-empirical approach to account for the eccentricity of the vertical force.

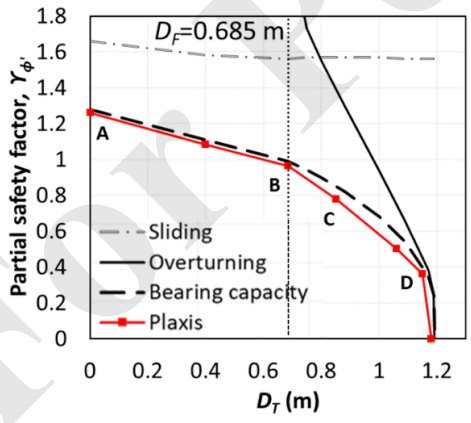

(a)

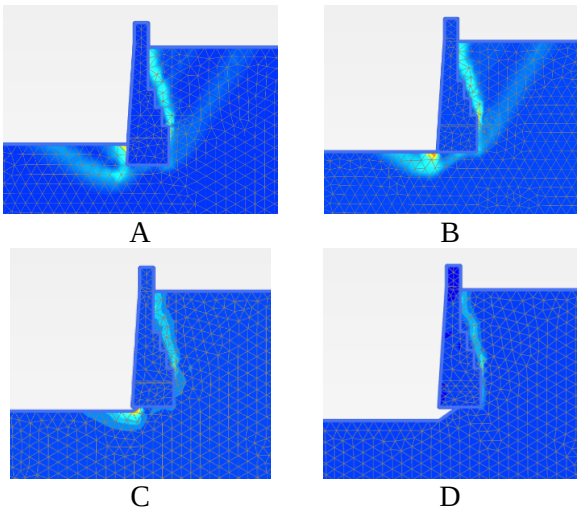

(b)

For Peer Review

Figure 5 Partial safety factor under scour for RW1 (a)closed-form solution and PLAXIS (b) incremental deviatoric strains contours show failure planes.

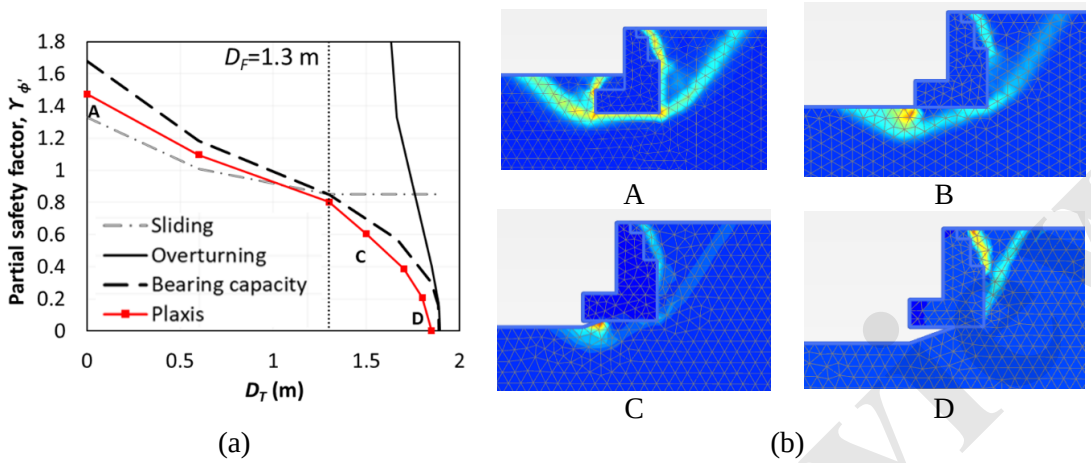

Figure 6 Partial safety factor under scour for RW2 (a)closed-form solution and PLAXIS (b) incremental deviatoric strains contours show failure planes.

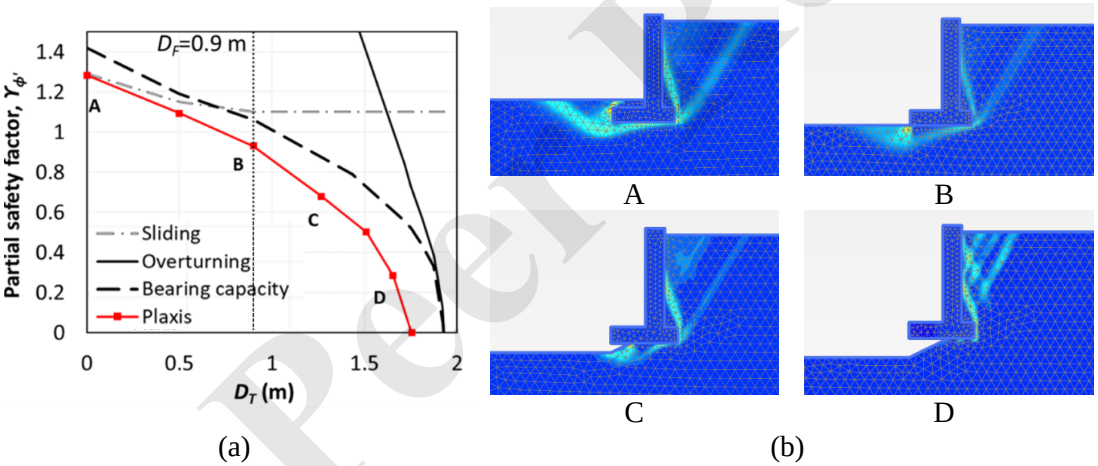

Figure 7 Partial safety factor under scour for RW3 (a) closed-form solution and PLAXIS (b) incremental deviatoric strains contours show failure planes.

6. Non-dimensional formulation

The partial safety factor for retaining walls subjected to scour is affected by several geometrical and mechanical parameters, including the wall height H, width of base B, width of toe B_t, embedded depth D_F, water depth H_w+D_F, friction angle of the base soil and retained soil ϕ', unit weight of the base soil and retained soil γ. In order to reduce the number of independent variables and highlight the most influential ones that control the problem, a

For Peer Review

dimensional analysis, using Buckingham's Pi theorem (Buckingham, 1914), is carried out. This approach is useful in parametric studies investigating various scenarios, by also preserving the relationships between parameters in a manner consistent with practical design principles. For instance, in the design of cantilever walls, the height-to-base width ratio typically falls within the range of 1 to 2. Table 2 illustrates the identified non-dimensional parameters and their range of variation, representing typical retaining wall designs in engineering practice (Sarıbaş and Erbatur 1996, Uray, Çarbaş et al. 2020, Kaveh, Biabani Hamedani et al. 2021). Table 2 illustrates the identified non-dimensional parameters and their range of variation, representing typical retaining wall designs in engineering practice (Sarıbaş and Erbatur 1996, Uray, Çarbaş et al. 2020, Kaveh, Biabani Hamedani et al. 2021). Regarding the water level, $(H_w+D_F)/H$ is assumed to vary between 0 and 0.6, where H_w+D_F represents the portion of the retaining wall below the water level. Accordingly, the relative footing depth D_F/H is assumed to fall within the range 0 to 0.3, and the normalized water depth H_w/H is likewise taken to vary between 0 and 0.3. It should be noted that higher relative water levels than those investigated may occur during extreme events leading to scour. However, considering a wider range of variation for H_w has no impact on the observed results.

Table 2 Non-dimensional in parameters controlling the problem and range of values.

Non-dimensional parameters		Symbol	Lower bound	Upper bound
Influencing parameters				
Π_1	Embedded depth of the wall//Height of the wall	D_F/H	0	0.3
Π_2	Width of the toe/width of the wall base	B_t/B	0	0.5
Π_3	Height of the wall /width of the wall base	H/B	1	2
Π_4	Friction angle of the base soil and retained soil	ϕ'	0.38	0.7
Π_5	Unit weight of the soil /Unit weight of water	γ/γ_w	1.6	2.8

For Peer Review

Π_6	Water level to foundation base level/Height of the wall	H_w/H	0	0.3
Π_7	Normalised scour demand	$D_T/D_{T,lim}$	0	1
Influenced variable				
	Partial factor under scour /partial factor at zero scour	$\gamma_{\phi\prime}/\gamma_{\phi\prime_0}$	0	1

To account for retaining walls characterized by a frictional behaviour at the wall-soil interface ($\delta > 0$), the interface friction angle is assumed equal to the soil's internal friction angle ($\delta = \phi'$). Moreover, to define the scour demand, the limit value of the scour depth is introduced, D_{Tlim}, defined as follows:

$$D_{Tlim} = D_F + (B_t + B_h/2) \cdot tan\phi' \quad (31)$$

The value of D_{Tlim} represents the condition where the foundation is undermined up to the centre of the heel. At this stage, the remaining soil beneath the heel cannot resist vertical gravitational forces corresponding to the retained soil, and thus stability is not possible regardless of the value of ϕ' , i.e., $\frac{\gamma_{\phi'}}{\gamma_{\phi'_0}} = 0$. The results obtained for the previously analysed case studies confirm this. The value of D_{Tlim} for RW1, RW2, and RW3 is 1.9 m, 1.9 m, and 1.2 m, respectively, which corresponds to the points where $\gamma_{\phi'}$=0 in Figure 5a, Figure 6a, and Figure 7a. As will be shown below, the proposed non-dimensional scour measure enables the identification of a single master curve, providing a unified, scaled representation onto which all data points, regardless of material or conditions.

In order to evaluate the influence of the non-dimensional parameters on the safety of retaining walls for different levels of scour, $N_{samples}$=6380 combinations of the non-dimensional parameters are generated, assuming uniform distributions between their respective lower and upper bounds. For each sample combination, corresponding to a wall-soil-water configuration, the normalised partial safety factor $\frac{\gamma_{\phi\prime}}{\gamma_{\phi\prime_0}}$ is determined for increasing values of the dimensionless scour depth $\frac{D_T}{D_{Tlim}}$ in the range from 0 to 1. The relationship

For Peer Review

between $\frac{\gamma_{\phi'}}{\gamma_{\phi'_0}}$ and $\frac{D_T}{D_{Tlim}}$ is then plotted, considering the combined effects of the multiple variables. Figure 8 illustrates the result of the analysis for the case of D_F/H=0 and D_F/H≥0. Despite significant variations in wall geometry, water depth, and soil properties, the reduction in the safety factor collapses onto a single master curve (red curve in Figure 8a). Notably, in the case of D_F/H=0 (a), the data exhibit minimal scatter from the master curve, which means that the reduction of the normalised partial factor is governed solely by the normalised scour depth and is independent of other non-dimensional parameters. The master curve can be approximated by Equation (32):

$$\frac{\gamma_{\phi'}}{\gamma_{\phi'_0}} = (1 - \frac{D_T}{D_{Tlim}})^{0.4} \quad (32)$$

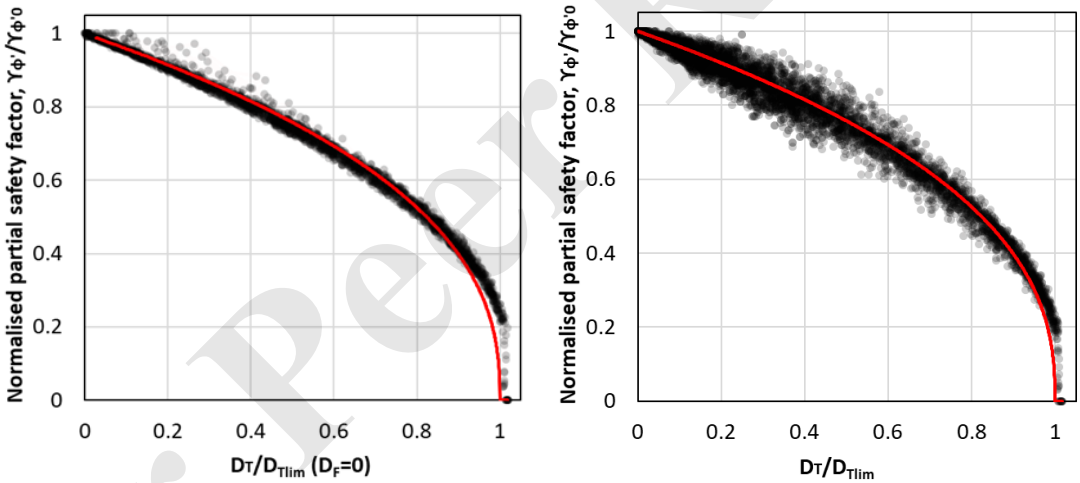

(a) (b)

Figure 8 The reduction of partial safety factor under progressive scour $\frac{D_T}{D_{Tlim}}$ for (a) D_F/H=0 (b) D_F/H≥0.

When D_F/H≥0 (Figure 8b), the variance of the data points and the scatter from the master curve increase. To investigate the source of variance under different levels of scour, global sensitivity analysis (Sobol 2001) is carried out to quantify the contribution of each variable and their interaction to the variance of the model output $\frac{\gamma_{\phi'}}{\gamma_{\phi'_0}}$. The sensitivity analysis is

For Peer Review

carried out at fixed values of the normalised scour depth, corresponding to values of $\frac{D_T}{D_{Tlim}}$ of 0.15, 0.3, 0.45, 0.6, 0.75, 0.9. At each scour level, the total output variance $V(\frac{\gamma_{\phi'}}{\gamma_{\phi'_0}})$ is evaluated by the variance of the expected value of $\frac{\gamma_{\phi'}}{\gamma_{\phi'_0}}$ conditioned on a fixed value of Π_i. The second-order effect, V_{ij}, is the joint effect of Π_i and Π_j minus the first-order effects for the same factor. The contribution of each input on the output variability is represented by Sobol indexes. The first-order Sobol index S_i quantifies the effect of input Π_i, while the total Sobol index S_{T_i} includes first-order effects of input Π_i plus all higher-order effects due to interaction.

The sensitivity analysis is conducted using the SobolGSA toolbox (Kucherenko 2013). The nondimensional factors are treated as independent random variables with uniform distributions over their respective ranges.

Figure 9 presents the sensitivity indices of Π_1,Π_2,...,Π_6 under different levels of scour. In general, it can be observed that these indices vary significantly with scour. In the early scour stage ($\frac{D_T}{D_{Tlim}}$< 0.15), D_F/H and H_w/H govern the output uncertainty, then their contribution gradually reduces. The total index for D_F/H stays above 0.2, while that for H_w/H drops to a negligible value after $\frac{D_T}{D_{Tlim}}$=0.3. In contrast, the indices for B_t/B, H/B, and ϕ' increase with scour and play secondary roles. The total sensitivity index of B_t/B rises from 0 to 0.3, then remains nearly flat with a slight decline to a value of 0.2. Meanwhile, the total sensitivity index of H/B consistently increases from 0 to 0.35 until $\frac{D_T}{D_{Tlim}}$=0.75. The increasing impact of H/B suggests the involvement of overturning failure, as higher H/B increases active pressure and the risk of overturning under the same scour conditions. The total sensitivity index of ϕ' increases from zero at the unscoured condition, peaks at 0.45, then decreases to 0.2, showing a hump trend. This reflects that ϕ' has double effects on the stability of retaining walls; a

For Peer Review

higher value of ϕ' increases the stability of the wall-soil system, but it can make it more unstable by steepening the inclination of the scour hole under the wall base. Compared with other variables, γ/γ_w has a negligible impact on the results and remains flat throughout.

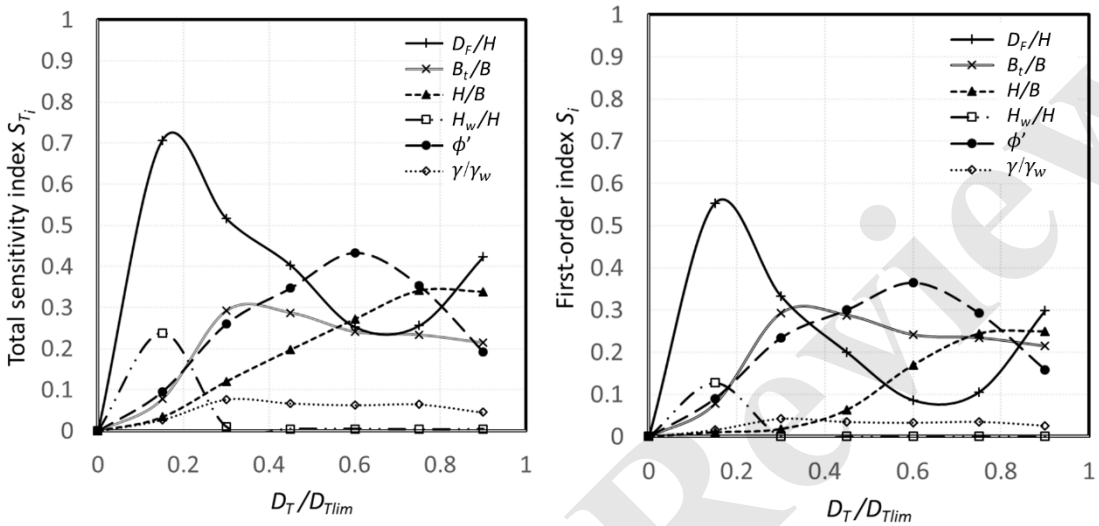

Figure 9 Sensitivity indices of non-dimensional variables under fix value of scour: (a) total sensitivity indices (b) first-order indices

The main outcome of the global sensitivity analysis is that many non-dimensional parameters have an impact on the output variance, and this impact changes with the scour depth. Thus, it is unpractical to attempt to derive an expression more sophisticated than Equation (32) to explicitly describe the effect of each parameter on the reduction of the safety factor. Rather than doing this, it is preferable to keep Equation (32) to estimate $\frac{\gamma_{\phi'}}{\gamma_{\phi'_0}}$ and derive a simple expression for quantifying its uncertainty. For this purpose, the relative squared errors (ε_i^2, i=1, 2,.., $N_{samples}$) and coefficient of variation (cov_s) are evaluated for increasing values of the normalized scour. We remind the reader that the relative squared error ε_i^2 of the i-th sample is defined as the square of the difference between the fitted values implied by equation (32) and the true value from the closed-form solution, divided by the true value. Figure 10 plots the relative squared errors ε_i^2 of the samples as a function of $\frac{D_T}{D_{Tlim}}$ and an estimate of cov_s^2

For Peer Review

obtained using a moving average method. It can be observed that the uncertainty cov_s^2 is zero when the scour is zero, increases progressively with scour until $\frac{D_T}{D_{Tlim}} = 0.5$, after which it is effectively constant. Based on this observation, a simplified expression can be derived for cov_s^2:

$$\mathrm{cov}_s^2 = min\left(0.06\frac{D_T}{D_{Tlim}}, 0.003\right) \quad (33)$$

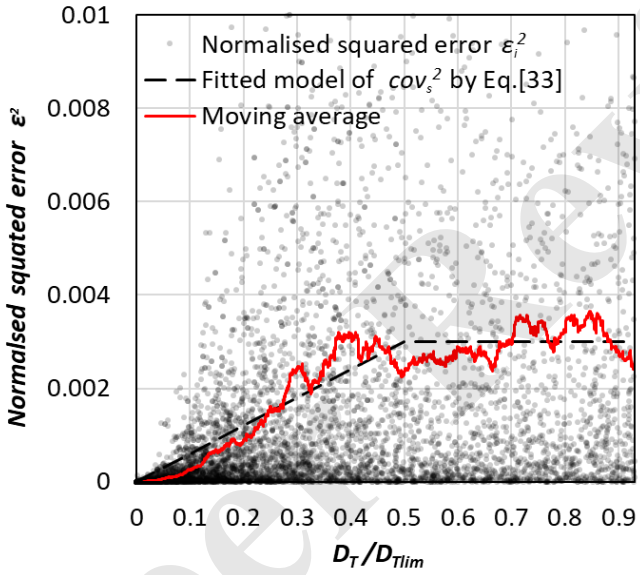

Figure 10 Variation of normalised squared error $\boldsymbol{\varepsilon^2}$ and $\mathbf{cov}_s^2$ with increasing scour.

7. Scour vulnerability model

In this section, a simplified model is derived for the scour vulnerability of retaining walls, based on reliability-based principles. This model links the probability of failure conditional to the scour level, by exploiting the closed-form expressions derived in the previous section for the mean reduction of the normalised safety factor due to scour and its coefficient of variation.

The safety factor $\gamma_{\phi'}$ of the retaining wall associated with the most critical failure mode is an uncertain quantity, whose variability depends on the design uncertainties and the additional uncertainty in capacity brought by scour. Assuming that $\gamma_{\phi'}$ is a random variable with

For Peer Review

lognormal distribution, mean value $E(\gamma_{\phi'})$ and coefficient of variation cov_Z, the probability of failure of the retaining wall can be expressed as:

$$P_F = \Phi(-\beta) \tag{34}$$

where Φ is the cumulative standard normal distribution and β is the Rosenblueth's and Esteva's reliability index (Rosenblueth and Esteva 1972), expressed by :

$$\beta = \frac{ln\, E(\gamma_{\phi'})}{cov_Z} \tag{35}$$

The uncertainty of the safety factor cov_Z combines the design uncertainty cov_0 and the additional uncertainty introduced by scour cov_s according to:

$$cov_Z = \sqrt{cov_0^2 + cov_s^2} \tag{36}$$

where uncertainty cov_s is quantified by equation (33), and the design uncertainty cov_0 is evaluated by a retaining wall with no scour. Similar to the general case, reliability index β_0 depends on the mean value of the design safety factor $E(\gamma_{\phi'_0})$ and the design uncertainty cov_0 through Rosenblueth's and Esteva's formula:

$$\beta_0 = \frac{E(\gamma_{\phi'_0})}{cov_0} \tag{37}$$

The design reliability β_0 depends on the level of overdesign of the retaining wall. It should be noted that the target failure probabilities of retaining walls are still very much unknown (He, Fenton and Griffiths 2022). According to Eurocode guidelines, a target reliability index β_0 of 3.8 is considered acceptable for designing retaining walls type structures under ultimate limit states (EN 1990:2002), and a nominal partial factor $\gamma_{\phi'_0}$ of 1.25 is recommended for the soil friction angle to have adequate safety margins in design under ultimate limit states (EN 1997). Assuming that the retaining walls was properly designed in compliance with the Eurocode requirements, with no overdesign, the design coefficient of variation cov_0 can be estimated as:

For Peer Review

$$cov_0 = \frac{ln\,\gamma_{\phi'_0}}{\beta_0} = \frac{ln\,1.25}{3.8} \approx 6\% \tag{38}$$

Respect to the design situation, scour reduces the reliability of the retaining wall as it reduces the wall's mean safety factor (as per equation (32)) and increases its uncertainty (as per equation (33)). It is convenient to rearrange equation (37) to highlight the contribution of the design reliability β_0. In formula:

$$\beta = \frac{ln\,E(\gamma_{\phi'})}{cov_Z} = \frac{\frac{ln\,E(\gamma_{\phi'_0})}{cov_0}\,cov_0 + ln\frac{E(\gamma_{\phi'})}{E(\gamma_{\phi'_0})}}{cov_Z} = \frac{\beta_0 \cdot cov_0 + ln\,E\left(\frac{\gamma_{\phi'}}{\gamma_{\phi'_0}}\right)}{\sqrt{cov_0^2 + cov_s^2}} \tag{39}$$

where we have accepted the approximation:

$$\frac{E(\gamma_{\phi'})}{E(\gamma_{\phi'_0})} \cong E\left(\frac{\gamma_{\phi'}}{\gamma_{\phi'_0}}\right) \tag{40}$$

The loss in reliability $\Delta\beta$ caused by scour can also be expressed in closed form by:

$$\Delta\beta = \beta - \beta_0 = \beta_0\left(\frac{cov_0}{\sqrt{cov_0^2 + cov_s^2}} - 1\right) + \frac{ln\,E\left(\frac{\gamma_{\phi'}}{\gamma_{\phi'_0}}\right)}{\sqrt{cov_0^2 + cov_s^2}} \tag{41}$$

Equation (39), together with (34), effectively provides an expression for the retaining wall's vulnerability as a function of the normalized scour depth $\frac{D_T}{D_{Tlim}}$:

$$P_F = \Phi(-\beta) = \Phi\left(-\frac{\beta_0 \cdot cov_0 + ln\,E\left(\frac{\gamma_{\phi'}}{\gamma_{\phi'_0}}\right)}{\sqrt{cov_0^2 + cov_s^2}}\right) \tag{42}$$

Equation (42) indicates that the scour vulnerability of retaining walls depends on four factors:

- the design reliability β_0 generally provided by (37) or conservatively assumed equal to 3.8;
- the design uncertainty cov_0 which can be assumed equal to 6% as per (38);
- the expected loss in safety factor $E\left(\frac{\gamma_{\phi'}}{\gamma_{\phi'_0}}\right)$ due to scour, quantified by (32);
- the additional uncertainty cov_s introduced by scour, quantified by (33)

For Peer Review

To illustrate the simplicity and practical effectiveness of the method, the vulnerability curves are derived for the three retaining walls with varying geometries shown in Figure 4. Table 3 lists the values of the wall and soil parameters needed to estimate D_{Tlim} which include the toe width, heel width, and embedded depth, extracted from the section drawing of the retaining walls, as well as the soil friction angle representative of the riverbed material, which is assumed. The value of β_0 can be assumed equal to 3.8 without performing any analysis of the retaining wall, based on the assumption that the wall satisfies the minimum reliability requirements. Alternatively, a more accurate β_0 can be estimated by the nominal partial safety factor $\gamma_{\phi'_0}$ in the case of no scour, which is evaluated by using the proposed closed-form method, together with cov_0 in equation (38) .

Table 3 Input parameters for estimating the probability of failure of retaining walls under scour

Case studies	Embedded depth D_F (m)	Soil friction angle ϕ' (°)	Toe width B_t (m)	Heel width B_h (m)	$\gamma_{\phi'_0}$	β_0
RW1	0.685	35	0	1.4	1.28	3.9
RW2	1.3	20	1	1.3	1.33	4.8
RW3	0.9	28	1.3	1.2	1.29	4.2

Figure 11 shows the vulnerability curves obtained for the selected case studies, conditional to the level of scour, as described by D_T or $\frac{D_T}{D_{Tlim}}$, in both the linear and semi-logarithmic scale. The curves in Figure 11a have been derived considering the values of β_0 reported in Table 3, corresponding to the actual values of $\gamma_{\phi'_0}$. The baseline vulnerability curve obtained for the Eurocode's target reliability β_0 = 3.8 is also plotted in the same figures, as dashed curves, for comparison. As expected, the probability of failure increases with scour and differs for the various walls. When the scour depth is expressed in dimensionless form, the vulnerability

For Peer Review

curves are closer to each other, and they differ only due to their different design reliability β_0, i.e. due to their different overdesign. Therefore, the baseline vulnerability curves, which have the same β_0 = 3.8, coincides in Figure 11b and represented by the red dashed curve (i.e., the Ref. curve).

The vulnerability curves on a logarithmic scale highlight the impact of scour on the probability of failure across several orders of magnitude (Figure 11c and Figure 11d). At zero scour depth, each retaining wall starts from a different value of probability of failure, with RW2 having the lowest value (1e^{-6}) and the reference case the highest value (7.5e^{-5}). The failure probability rises sharply by several orders of magnitude due to scour: in the reference case, the failure probability increases by one, two, and three orders of magnitude for values of the normalised scour level of 0.07, 0.15, and 0.28. It is also worth to observe that the failure probability reaches the value of 1 when $\frac{D_T}{D_{Tlim}}$ approaches 0.7, regardless of the initial value of β_0. Use of the reference curve is recommended in absence of more detailed information on the overdesign level, since it provides conservative estimates of the vulnerability.

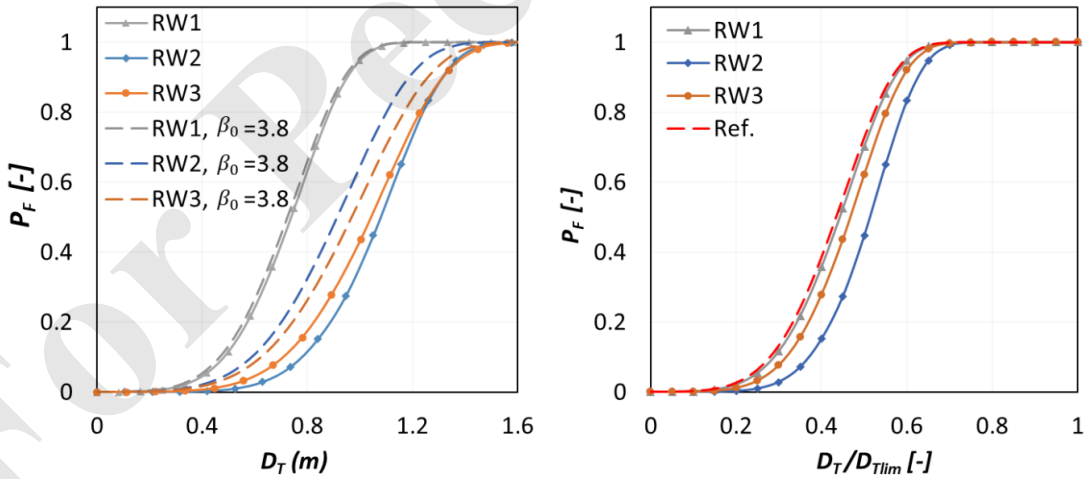

(a) (b)

For Peer Review

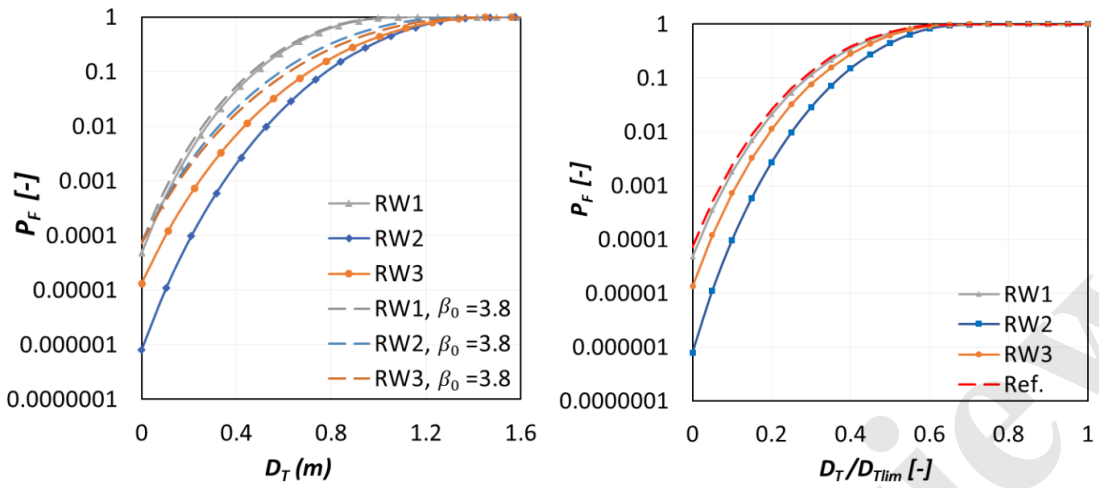

(c) (d)

Figure 11 Vulnerability curves of the retaining walls (a) dimensional scour presentation (b) non-dimensional scour presentation (c) dimensional scour on a logarithmic scale of P_F (d) non-dimensional scour on a logarithmic scale of P_F.

8. Conclusion

This study has introduced a novel, simplified analytical approach to evaluate the safety of retaining walls under scour conditions, effectively addressing a key gap in the assessment of their vulnerability. The analytical approach commonly used for the stability analysis of retaining walls has been extended in this study to account for the effects of scour on the most critical failure mechanisms—namely, overturning, sliding, and loss of base support. Closed-form expressions have been developed and validated against numerical modelling using three representative retaining walls in the UK transport network, showing good accuracy across a range of wall geometries, soil properties, and hydraulic conditions. Moreover, by expressing the problem in dimensionless terms and applying global sensitivity analysis, the study has proposed a nondimensional scour measure, which enables identification of a single master curve that provides a unified and scaled representation of the safety factor reduction, regardless of the variation in wall configurations, water depths, and riverbed and soil properties. Finally, a model for the scour vulnerability of retaining walls has been developed

For Peer Review

based on a reliability-based framework, by exploiting the closed-form expressions for the mean safety factor reduction and its coefficient of variation.

The proposed method enables rapid estimation of scour vulnerability of retaining walls using basic input parameters, making it suitable for infrastructure asset management and prioritizing maintenance and intervention strategies in flood-prone areas. Future work will extend this method to other retaining wall typologies (e.g. gabion walls, diaphragm walls and anchored walls) and will also provide practical guidelines for implementation in scour risk assessment and management procedures.

Acknowledgements: this financial support of National Highways through the project 'Foundations: improving risk assessment and prioritisation processes for management of scour at structures' is greatly acknowledged. This project is a collaboration with Connected Places Catapult, funded by the Engineering and Physical Sciences Research Council's Innovation Launchpad Network+ Researcher in Residence scheme (grant numbers EP/W037009/1, EP/X528493/1).

References

ACI (2011). Building Code Requirements for Structural Concrete (ACI 318-11), American Concrete Institute.

Argyroudis, S. A. and S. A. Mitoulis (2021). "Vulnerability of bridges to individual and multiple hazards- floods and earthquakes." Reliability Engineering & System Safety **210**: 107564.

Buckingham, E. (1914). "On physically similar systems; illustrations of the use of dimensional equations." Physical Review 4(4): 345–376.

Cely Calixto, N. J., A. Galvis Castaño and G. A. Carrillo Soto (2023). "Evaluation of Local Scour along the Base of Longitudinal Training Walls." Water 15(22): 4001.

Cerema (2019). Analyse de risque des ponts en site affouillable (in French). Collection: Références.

CIRIA (2015). Manual on scour at bridges and other hydraulic structures, second edition (C742).

CIRIA (2021). Manual on scour at bridges and other hydraulic structures - supplementary guide (SP171).

For Peer Review

Daryani, K. E., and Mohamad, H. (2014). System reliability-based analysis of cantilever retaining walls embedded in granular soils. *Georisk: Assessment and Management of Risk for Engineered Systems and Geohazards*, *8*(3), 192-201.

EN (1990:2002). Eurocode: Basis of structural design.

EN (1997). Eurocode 7 geotechnical design—part 1: general rules.

Fael, C. S., G. Simarro-Grande, J. P. Martín-Vide and A. H. Cardoso (2006). "Local scour at vertical-wall abutments under clear-water flow conditions." Water Resources Research **42**.

Hansen, J. B. (1970). "A revised and extended formula for bearing capacity."

He, P., G. A. Fenton, and D. V. Griffiths (2023). "Calibration of resistance factors for gravity retaining walls." Georisk: Assessment and Management of Risk for Engineered Systems and Geohazards, **17**(3): 586-594.

Heydari, N. and P. Diplas (2020). "Flow dynamics in the vicinity of a gravel embedded vertical retaining wall: conditions corresponding to the initial stages of local erosion." Environmental Fluid Mechanics **20**(1): 203-225.

Huang, C.-C. (2017). "Failure mechanisms of steep-faced geosynthetic-reinforced retaining walls subjected to toe scouring." Marine Georesources & Geotechnology **35**(8): 1099-1110.

Kaveh, A., K. Biabani Hamedani and A. Zaerreza (2021). "A set theoretical shuffled shepherd optimization algorithm for optimal design of cantilever retaining wall structures." Engineering with Computers **37**(4): 3265-3282.

Khosronejad, A., P. Diplas, D. Angelidis, Z. Zhang, N. Heydari and F. Sotiropoulos (2020). "Scour depth prediction at the base of longitudinal walls: a combined experimental, numerical, and field study." Environmental Fluid Mechanics **20**(2): 459-478.

Kucherenko, S. (2013). "SobolHDMR: a general-purpose modeling software." Methods Mol Biol **1073**: 191-224.

Lancellotta, R. (2002). "Analytical solution of passive earth pressure." Géotechnique **52**(8): 617-619.

McKelvey, J. A. III (2011). "Lessons learned from failures: The wall of shame." In Geo-Frontiers 2011: Advances in Geotechnical Engineering, 3235–3244.

NationalHighways (2024). CS 469 - Management of scour and other hydraulic actions at highway structures.

PLAXIS (2020). PLAXIS 3D Reference manual CONNECTION edition V20.03.

Rosenblueth, E. and L. Esteva (1972). Reliability Basis for Some Mexican Codes.

For Peer Review

Sarıbaş, A. and F. Erbatur (1996). "Optimization and sensitivity of retaining structures." Journal of Geotechnical Engineering **122**(8): 649-656.

Scozzese, F., E. Tubaldi and A. Dall'Asta (2023). "Damage metrics for masonry bridges under scour scenarios." Engineering Structures **296**: 116914.

Sobol, I. M. (2001). "Global sensitivity indices for nonlinear mathematical models and their Monte Carlo estimates." Mathematics and Computers in Simulation **55**(1): 271-280.

Sotiropoulos, F. and P. Diplas (2017). "Scour at the base of retaining walls and other longitudinal structures: Final report." NCHRP, Transportation Research Board, The National Academies.

Theinat, A. K., R. Salgado, M. Prezzi and V. A. Sakleshpur (2024). "Stability and factor of safety of gravity-retaining structures using the strength reduction method." J Journal of Geotechnical and Geoenvironmental Engineering.

Tubaldi, E., C. J. White, E. Patelli, S. A. Mitoulis, G. de Almeida, J. Brown, M. Cranston, M. Hardman, E. Koursari, R. Lamb, H. McDonald, R. Mathews, R. Newell, A. Pizarro, M. Roca and D. Zonta (2022). "Invited perspectives: Challenges and future directions in improving bridge flood resilience." Nat. Hazards Earth Syst. Sci. **22**(3): 795-812.

Uray, E., S. Çarbaş, İ. H. Erkan and M. Olgun (2020). "Investigation of optimal designs for concrete cantilever retaining walls in different soils." Challenge Journal of Concrete Research Letters; Vol 11, No 2 (2020)DO - 10.20528/cjcrl.2020.02.003.

Vesić, A. S. (1973). "Analysis of Ultimate Loads of Shallow Foundations." Journal of the Soil Mechanics and Foundations Division **99**(1): 45-73.

For Peer Review

Appendix 1: Earth pressures for cantilever walls adjacent to river and under scour actions

A1.1 Active thrust

Figure A-1 shows an ideal model of retaining wall and the location of active pressure, which is assumed to be applied at the edge of the heel.

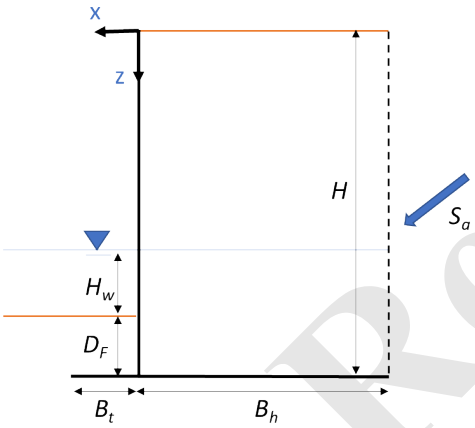

Figure A-1 Ideal model for active pressure of retaining wall adjacent to river

The horizontal and vertical components of active thrust are calculated by integrating the horizontal total stress σ_x and the tangential stress τ_{xz} respectively along the height H of the wall.

$$S_{ah} = \int_0^H (\sigma'_x + u_w)\, dz = \frac{1}{2} k_a \gamma H^2 + \frac{1}{2}(1 - k_a)\gamma_w (H_w + D_F)^2 \quad \text{(A1-1)}$$

$$S_{av} = \int_0^H \tau_{xz}\, dz = \int_0^H k_a^* \sigma'_z\, dz = \frac{1}{2} k_a^* \gamma H^2 - \frac{1}{2} k_a^* \gamma_w (H_w + D_F)^2 \quad \text{(A1-2)}$$

$$k_a = \frac{\cos\delta}{1 + \sin\phi'} \left(\cos\delta - \sqrt{\sin^2\phi' - \sin^2\delta}\right) e^{-2\theta \tan\phi'} \quad \text{(A1-3)}$$

For Peer Review

$$k_a^* = \tan\delta\, k_a \tag{A1-4}$$

$$2\theta = \operatorname{asin}\left(\frac{\sin\delta}{\sin\phi'}\right) - \delta \tag{A1-5}$$

$$u_w = \gamma_w\left[z - \left(H - (H_w + D_F)\right)\right] \tag{A1-6}$$

A1.2: Passive thrust

Figure A-2 shows the retaining wall and the location of passive pressure, which is assumed to be applied at the edge of the toe.

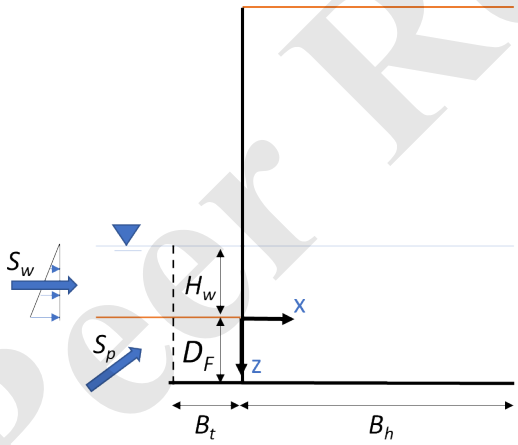

Figure A-2 Ideal model for passive pressure of retaining wall adjacent to river

The horizontal and vertical components of passive thrust are calculated by integrating the horizontal total stress σ_x and the tangential stress τ_{xz} respectively along t embedded depth and the height of water.

$$S_{ph} = \int_0^{D_F} \sigma_x\, dz = \frac{1}{2}(\gamma - \gamma_w)k_p {D_F}^2 + \left(\frac{1}{2}\gamma_w {D_F}^2 + \gamma_w H_w D_F\right) \tag{A1-7}$$

For Peer Review

$$S_{pv} = \int_0^{D_F} \tau_{xz}\, dz = \int_0^{D_F} k_p^*(\sigma_z - u_w)\, dz = \frac{1}{2}(\gamma - \gamma_w) k_p^* {D_F}^2 \quad \text{(A1-8)}$$

$$k_p = \frac{\cos\delta}{1 - \sin\phi'}\left(\cos\delta + \sqrt{\sin^2\phi' - \sin^2\delta}\right) e^{2\theta \tan\phi'} \quad \text{(A1-9)}$$

$$k_p^* = \tan\delta\, k_p \quad \text{(A1-10)}$$

$$2\theta = \operatorname{asin}\left(\frac{\sin\delta}{\sin\phi'}\right) + \delta \quad \text{(A1-11)}$$

$$u_w = \gamma_w(H_w + z) \quad \text{(A1-12)}$$

Appendix 2: Overturning failure of retaining wall under progressive scour

For $D_T \leq D_F$, the overturning point is at the edge of the toe on the water side, and the overturning factor given by:

$$f_{ov} = \frac{S_{ah,1}\frac{H}{3} + S_{ah,2}\frac{H_w + D_F}{3} + U\frac{B_t + B_h}{2}}{S_{av}(B_h + B_t) + W_h\left(\frac{B_h}{2} + B_t\right) + W_t\left(\frac{B_t}{2}\right) + S_w\left(\frac{H_w + D_T}{3} + D_F'\right) + S_{ph,1}\frac{D_F'}{3} + S_{ph,2}\frac{D_F'}{2}} \quad \text{(A2-1)}$$

When $D_T > D_F$ and $0 < W_s \leq B_t/2$, the foundation is exposed, and the passive pressure is zero. The overturning point moves toward the heel but does not exceed the centre of the toe. This shift changes the overturning arm for active pressure, buoyancy force, and the vertical resultant forces on wall base. The expression of the overturning factor becomes:

For Peer Review

$$f_{ov} = \frac{S_{ah,1}\frac{H}{3} + S_{ah,2}\frac{H_w + D_F}{3} + U|W_s - \frac{B_t + B_h}{2}|}{S_{av}|B_h + B_t - W_s| + W_h|\frac{B_h}{2} + B_t - W_s| + W_t|\frac{B_t}{2} - W_s| + S_w\left(\frac{H_w + D_F}{3}\right)} \quad \text{(A2-2)}$$

When $D_T > D_F$ and $B_t/2 < W_s \leq B_t/2 + B_h/2$, the overturning point moves further toward the heel, causing W_t to act as a destabilising force. The overturning factor is:

$$f_{ov} = \frac{S_{ah,1}\frac{H}{3} + S_{ah,2}\frac{H_w + D_F}{3} + W_t|\frac{B_t}{2} - W_s| + U|W_s - \frac{B_t + B_h}{2}|}{S_{av}|B_h + B_t - W_s| + W_h|\frac{B_h}{2} + B_t - W_s| + S_w\left(\frac{H_w + D_F}{3}\right)} \quad \text{(A2-3)}$$

When $D_T > D_F$ and $(B_t + B_h)/2 \leq W_s < B_t + B_h/2$, the overturning point moves beyond the centre of the foundation, causing the buoyancy to act as a stabilization force. Thus, the overturning factor is given by:

$$f_{ov} = \frac{S_{ah,1}\frac{H}{3} + S_{ah,2}\frac{H_w + D_F}{3} + W_t|\frac{B_t}{2} - W_s|}{S_{av}|B_h + B_t - W_s| + W_h|\frac{B_h}{2} + B_t - W_s| + S_w\left(\frac{H_w + D_F}{3}\right) + U|W_s - \frac{B_t + B_h}{2}|} \quad \text{(A2-4)}$$

Finally, when $D_T > D_F$ and $W_s \geq B_t + B_h/2$, the overturning point moves beyond the centre of the heel, and W_h becomes a destabilizing force.

$$f_{ov} = \frac{S_{ah,1}\frac{H}{3} + S_{ah,2}\frac{H_w + D_F}{3} + W_t|\frac{B_t}{2} - W_s| + W_h|\frac{B_h}{2} + B_t - W_s|}{S_{av}|B_h + B_t - W_s| + S_w\left(\frac{H_w + D_F}{3}\right) + U|W_s - \frac{B_t + B_h}{2}|} \quad \text{(A2-5)}$$

For Peer Review

Vulnerability Model for Cantilever Retaining Walls Subject to Scour

Lanting Wei[1], Alessandro Tarantino[2], Enrico Tubaldi[3*], Hamed Moghaddasi[4], and Daniele Zonta[5]

[1]Dept. of Civil and Environmental Engineering, Univ. of Strathclyde, Glasgow, UK; [2]Dept. of Civil and Environmental Engineering, Univ. of Strathclyde, Glasgow, UK; [3]Dept. of Civil and Environmental Engineering, Univ. of Strathclyde, Glasgow, UK; Email: enrico.tubaldi@strath.ac.uk; [4]Dept. of Civil and Environmental Engineering, Univ. of Strathclyde., Glasgow, UK;[5]Dept. of Civil, Environmental and Mechanical Engineering, Univ. of Trento, Via Mesiano, Trento, Italy*

For Peer Review

Vulnerability Model for Cantilever Retaining Walls Subject to Scour

Abstract: Retaining walls are widely used to stabilize slopes and support infrastructure such as bridge abutments, culverts, and roads over or adjacent to waterways. These structures can be susceptible to scour-induced erosion and undermining at their toe, which can lead to significant damage and collapse. This paper presents a comprehensive yet simplified analytical formulation to evaluate the reduction in retaining wall capacity caused by scour. First, a model is proposed to describe the scour process at retaining walls. Based on this model, the degradation of retaining wall capacity is formulated by considering various potential failure modes. The proposed formulation, validated against numerical simulations using PLAXIS, is non-dimensionalised to derive simple expressions for describing the effect of scour across different wall geometries, soil properties, and water depths. A simplified approach is then introduced to estimate the scour vulnerability of retaining walls, expressing the conditional probability of wall failure with increasing scour levels. The study provides a practical tool for engineers and infrastructure asset managers to support rapid risk prioritization of retaining walls exposed to scour, highlighting the most critical parameters influencing the vulnerability of these structures.

Keywords: Scour; Vulnerability; Retaining walls; Closed-form solution; Flooding.

1.Introduction

Retaining walls are commonly employed to stabilize slopes and support transport infrastructure elements such as bridge abutments, culverts, and over or adjacent to waterways. These structures are susceptible to scour-induced erosion and toe undermining, which can lead to significant damage and structural failure (Khosronejad, Diplas et al. 2020). Scour at the base of retaining walls is typically associated with four mechanisms: (i) general scour, resulting from the natural evolution of waterways that lowers the elevation of river channels; (ii) constriction scour, where a reduction in river width increases flow velocity within the channel; (iii) local scour, which occurs at the leading edge of retaining walls due to high-energy turbulence; and (iv) bend scour, which affects retaining walls along outer banks of meandering rivers due to sudden changes in flow velocity and direction at bends. The

For Peer Review

interaction of these scour mechanisms can significantly increase the risk of retaining wall failure (Heydari and Diplas 2020). This risk can also be significantly exacerbated by the ageing of these structures and the intensification of extreme weather events and floods due to climate change.

While the vulnerability of bridges to scour has been extensively investigated (Argyroudis and Mitoulis 2021, Tubaldi, White et al. 2022, Scozzese, Tubaldi et al. 2023), research on the vulnerability of retaining walls remains limited. Guidelines and standards on scour risk assessment, such as CIRA manuals SP171 and C742 (CIRIA 2015, CIRIA 2021), CS 469 (NationalHighways 2024) and French guidelines (Cerema 2019) provide limited information on the evaluation of the scour risk of retaining walls. Furthermore, scour is frequently overlooked in the design of retaining walls located adjacent to watercourses, a practice that has been associated with catastrophic failures (McKelvey, 2011). Thus, there is a need to develop scour vulnerability and risk assessment procedures accounting for the specific features of these structures.

The hydraulic processes responsible for scour at the base of longitudinal training walls differ from those acting on bridge piers. A key distinction is that, along retaining walls, lateral flow typically generates elongated scour patterns, whereas pier scour is dominated by downflow and the formation of a horseshoe vortex at the upstream face. Some studies have examined the hydraulic aspects of the problem, especially the evaluation of the scour depth along walls (Heydari and Diplas 2020). Different approaches have been proposed for estimating the scour depth in longitudinal structures through experimental flume studies and empirical formulations (Fael, Simarro-Grande et al. 2006, Khosronejad, Diplas et al. 2020, Calixto, Castaño et al. 2023, Sotiropoulos and Diplas 2017). It has been found that the development of a scour hole is influenced by a wide range of hydraulic, geotechnical factors and geometry of

For Peer Review

the problem, including the wall's orientation relative to the approaching flow, local flow velocity and turbulence intensity, sediment transport capacity, and the properties of the riverbed material (Calixto, Castaño et al. 2023, Sotiropoulos and Diplas 2017). Other studies, discussed in Huang (2017), have investigated the failure mechanisms for reinforced retaining walls under toe scouring action, with primary emphasis on coastal settings. However, despite the efforts made on understanding the hydraulic processes and evaluating the scour depth along retaining walls, the influence of scour on the stability of retaining walls has not received sufficient attention. To the best of the author's knowledge, no previous studies have explicitly proposed models to describe the scour vulnerability of these structures.

The evaluation of the impact of scour on the capacity of retaining walls is a complex task, which must consider the likelihood of occurrence of several failure modes, namely the exceedance of the foundation bearing capacity, the sliding at the base of the foundation, and the structure overturning (Theinat et al., 2024). The geometry of the walls, the properties (e.g. friction angle and cohesion) of the backfill and base soil, as well as the water level, all play an important role in the vulnerability assessment and affect both the demand and the capacity. Although advanced numerical models can be developed for investigating the vulnerability of retaining walls, there is a need for vulnerability models which are simple enough to be embedded in standards and used for identifying those walls that are more vulnerable to scour.

This study illustrates a simple yet accurate analytical formulation for evaluating the effect of scour on the safety factor of retaining walls. The proposed formulation uses Lancellotta's earth pressure coefficients to calculate active and passive thrusts (Lancellotta 2002) accounting for wall friction and the bearing capacity model of Hansen and Vesić (Hansen 1970, Vesić 1973), with both models further extended to consider the effect of scour. Validated against the results of advanced numerical analysis of retaining walls in PLAXIS

For Peer Review

(PLAXIS 2020), the proposed formulation accounts for the various possible limit states that could result in wall failure due to scour.

The analytical formulation is non-dimensionalised, and global sensitivity analysis is performed with the aim of deriving a simple curve that describes the reduction in the partial safety factor with increasing scour levels, accounting for wall geometry, soil properties, and water height. The proposed curve can be used for the preliminary assessment of retaining walls and the identification of the most critical parameters that control the wall's safety. In the last part of the paper, fragility functions are developed to describe the conditional probability of wall failure with increasing scour levels.

The rest of the paper is organised as follows. A description of the various actions, resisting mechanisms and limit state functions that underpin the proposed closed-form formulation for the evaluation of the impact of scour on the safety of retaining walls is provided first. Following this, the validation of the formulation is presented, using advanced numerical models developed in PLAXIS (PLAXIS 2020) for three case studies. Next, the paper introduces the non-dimensional formulation that describes the reduction in safety of retaining walls with increasing levels of normalised scour depth, along with the results from global sensitivity analyses that highlight the influence of model parameters on the non-dimensional outcomes. The development of simplified fragility functions for retaining walls exposed to scour is then presented, followed by a conclusion section.

2. Actions and resisting mechanisms for retaining walls exposed to scour

2.1 Problem geometry

Figure 1 illustrates the geometry of the idealised model used to represent both cantilever and gravity retaining walls.

For Peer Review

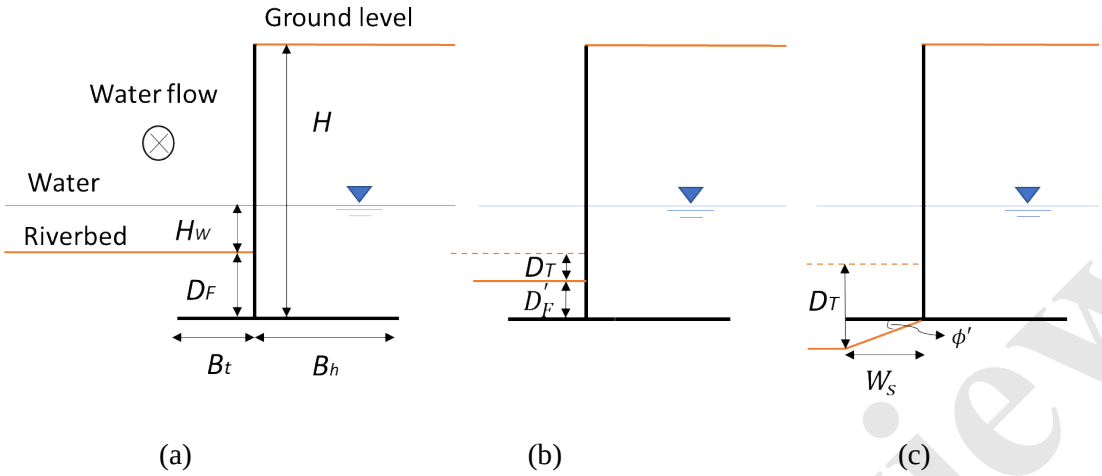

Figure 1 Idealised model of retaining wall: (a) case of no scour (b) scour in stage 1: $D_T \leq D_F$ (c) scour in stage 2: $D_T > D_F$

The wall has a total height H, and a foundation width of B, which is made up of the toe length B_t and the heel length B_h. The wall is embedded into the riverbed, with D_F representing the depth from the riverbed surface to the base of the foundation. The water height H_w refers to the vertical distance from the riverbed to the water surface.

Scour is assumed to progress in two stages: first, the riverbed soil is eroded uniformly (Figure 1b) until the base of the foundation is reached and the toe is fully exposed. Then, the soil at the base of the foundation is undermined, from the edge of the toe towards the heel, as illustrated in Figure 1c. The maximum depth of scour below the riverbed is denoted as D_T. During the first stage (i.e., $D_T \leq D_F$ in Figure 1b), increasing levels of scour correspond to a reduction of the embedded depth:

$$D'_F = \max(0, D_F - D_T) \quad (1)$$

For Peer Review

During the second stage (i.e, D_T>D_F in Figure 1c), scour undermines the bottom of the foundation and progresses horizontally from the toe to the heel, with a width W_s defined by Equation (2).

$$W_s = \frac{D_T - D_F}{tan\phi'} \quad (2)$$

where the angle of inclination of the scour hole is assumed equal to the effective soil friction angle ϕ'. This assumption idealizes the scour slope as being controlled only by riverbed material properties. In reality, scour slope angles are also influenced by other factors including wall angles relative to the approach flow, flow velocity and turbulence, sediment transport capacity, and time dependent scour development etc. (Calixto, Castaño et al. 2023, Sotiropoulos and Diplas 2017). The adopted scour angle is therefore intended as a simplified representation for modelling purposes and should be interpreted within the limitations of this assumption.

Figure 2 illustrates actions and resisting mechanisms for retaining walls exposed to scour. The wall is subjected to the active thrust S_a at the edge of the heel and the passive thrust S_p at the edge of the toe. The soil exerts a gravity force W_h and W_t on the heel and toe, respectively. As a result of these actions, the base is subject to a total vertical force N and a total horizontal force T. The total vertical force N is applied with an eccentricity e, measured from the centre of the effective foundation width B'- the portion of the base still in contact with the soil after scour. The maximum horizontal force T_{lim} and the maximum vertical force Q_{lim}, acting beneath the wall base, represent the thresholds beyond which sliding and bearing capacity failures are initiated, respectively.

For Peer Review

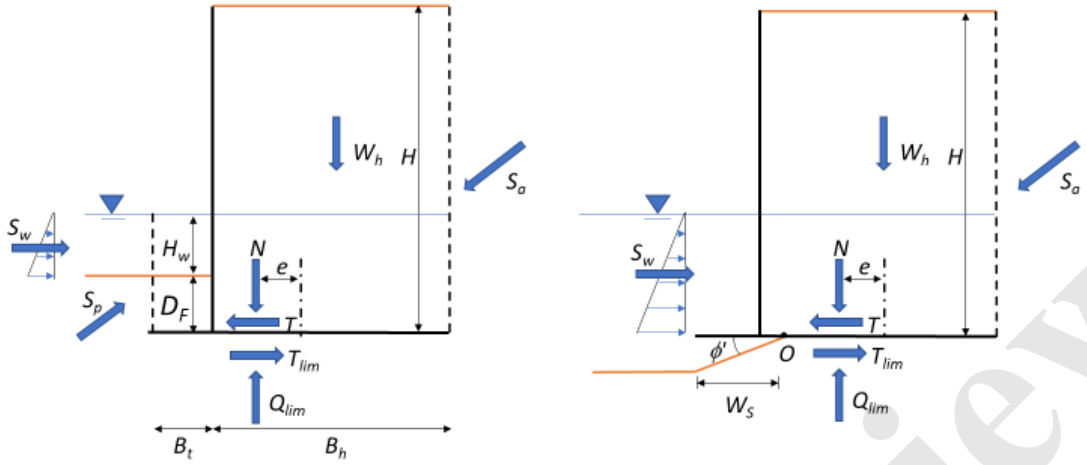

(a) (b)

Figure 2. Sketch of a cantilever wall for the case of (a) no scour (b) scour undermining the foundation.

Failure of retaining walls can occur through three mechanisms. Bearing capacity failure occurs when the applied normal force N exceeds the limiting capacity $Q_{lim.}$ Sliding failure takes place when the driving shear force T surpasses the available resistance T_{lim}. Overturning failure happens when the destabilizing moment exceeds the stabilizing moment, with both these moments measured with respect to the point of intersection between the scour hole and the foundation base (i.e., point O in Figure 2b).

2.2 Active and passive thrusts

Accurate estimation of the active thrust S_a and passive thrust S_p is crucial for assessing the stability of retaining walls under all failure mechanisms. The earth pressures should also account for the impact of water. On the backfill side, water adds horizontal hydrostatic force to the active earth pressure on the lower portion of the wall. On the riverside, with water above the riverbed, the weight of water increases the passive pressure. The earth pressures are also affected by scour. With wall friction considered, scour changes the vertical component

For Peer Review

of passive pressure, therefore influencing sliding resistance, overturning moments, and the overall geotechnical demand.

The active thrust S_a is given in Equations (3)-(5) and the passive thrust S_p is in Equations (6)-(8); their expressions are based on the coefficient k_a for active thrust and k_p for passive thrust derived using the lower bound theorem of plasticity (Lancellotta 2002). Each earth pressure consists of two parts, with a different pressure distribution and point of application, requiring separate consideration during moment equilibrium calculations for accurate stability assessment. For active pressure, $S_{ah,1}$ is the active pressure from the retained soil, whereas $S_{ah,2}$ accounts for hydrostatic water pressure, which acts partially on the lower portion of the soil-wall system. For passive pressure, $S_{ph,1}$ is the passive pressure, and $S_{ph,2}$ represents the weight of overlying water forming a rectangular pressure distribution. Both passive pressure components change with scour. Due to friction at soil-wall interface, the effective vertical component of earth pressure forms an angle δ with the effective horizontal component, where δ is assumed equal to soil friction angle ϕ'. It should be noted that the soil–wall interface is actually a soil–soil interface, since the soil above the heel is treated as an integral part of the retaining wall. The development of the expressions for earth pressures is illustrated in Appendix 1.

$$S_{ah} = \underbrace{\frac{1}{2} k_a \gamma H^2}_{S_{ah.1}} + \underbrace{\frac{1}{2}(1 - k_a)\gamma_w (H_w + D_F)^2}_{S_{ah.2}} \tag{3}$$

$$k_a = (1 - \sin\phi')e^{-\left(\frac{\pi}{2} - \phi'\right)\tan\phi'} \tag{4}$$

$$S_{av} = \frac{1}{2}\tan\phi' \, k_a \gamma H^2 - \frac{1}{2}\tan\phi' \, k_a \gamma_w (H_w + D_F)^2 \tag{5}$$

For Peer Review

$$S_{ph} = \underbrace{\frac{1}{2}\gamma k_p D_F'^2 + \frac{1}{2}(1-k_p)\gamma_w D_F'^2}_{S_{ph,1}} + \underbrace{\gamma_w (H_w + D_F - D_F')D'_F}_{S_{ph,2}} \quad (6)$$

$$k_p = (1+\sin\phi')e^{\left(\frac{\pi}{2}+\phi'\right)\tan\phi'} \quad (7)$$

$$S_{pv} = \frac{1}{2}(\gamma - \gamma_w)k_p^* = \tan\phi'\, k_p D_F'^2 \quad (8)$$

2.3 Bearing capacity

Scour impacts the bearing capacity by reducing the embedded depth and the effective soil-foundation interface, and this in turn changes the eccentricity and the inclination of the resultant load on the riverbed. The change in eccentricity further reduces the effective width of the foundation. To capture these effects, the bearing capacity formulation is developed for the three scenarios illustrated in Figure 1. The riverbed soil is assumed to be cohesionless and homogeneous, with its effective friction angle remaining unchanged by scour.

In the absence of scour, the effective bearing capacity q'_{lim} is given by the following expression based on Hansen and Vesić's approach (Hansen 1970, Vesić 1973):

$$q'_{lim} = \frac{1}{2}\gamma B' N_\gamma i_\gamma + \gamma D_F N_q i_q \quad (9)$$

where B' is the effective foundation width, given by:

$$B' = B_h + B_t - 2e \quad (10)$$

In Equation (10), N_q and N_γ are dimensionless factors depending on the friction angle of the

For Peer Review

soil, and i_q and i_γ are surcharge inclination angles depending on the ratio between the horizontal and vertical force, *T* and *N*.

$$N_q = \frac{1+\sin\phi'}{1-\sin\phi'}\exp(\pi\tan\phi') \tag{11}$$

$$N_\gamma = 1.5\left(N_q - 1\right)\tan\phi' \tag{12}$$

$$i_q = \left(1-\frac{T}{N}\right)^2 \tag{13}$$

$$i_\gamma = \left(1-\frac{T}{N}\right)^3 \tag{14}$$

For low scour depths such that the foundation is not undermined ($D_T \leq D_F$), q'_{lim} is given by:

$$q'_{lim} = \frac{1}{2}\gamma B' N_\gamma i_\gamma + \gamma D F' N_q i_q \tag{15}$$

When scour reaches the base of the foundation ($D_T > D_F$), undermining a portion W_s of the foundation, q'_{lim} is given by:

$$q'_{lim} = \frac{1}{2}\gamma B' N_\gamma i_\gamma \tag{16}$$

$$B' = (B_h + B_t - W_s) - 2e \tag{17}$$

A positive eccentricity *e* means the resultant force *N* is positioned to the left of the effective foundation centre. When scour occurs but the foundation is not undermined (i.e. $D_T \leq D_F$), moment equilibrium results in an eccentricity with respect to the mid-point of the effective

For Peer Review

foundation by Equation (18).

$$e = \frac{W_t \frac{B_h}{2} + S_{ah,1} \frac{H}{3} + S_{ah,2} \frac{H_w + D_F}{3}}{W_t + W_h + S_{av} - S_{pv} - U} - \frac{W_h \frac{B_t}{2} + S_{av}\left(\frac{B_h + B_t}{2}\right) + S_{ph,1} \frac{D'_F}{3} + S_{ph,2} \frac{D'_F}{2} + S_{pv}\left(\frac{B_h + B_t}{2}\right) + S_w\left(\frac{H_w + D_T}{3} + D'_F\right)}{W_t + W_h + S_{av} - S_{pv} - U} \quad (18)$$

When scour undermines the foundation (i.e., $D_T > D_F$ and $Ws > 0$), moment equilibrium introduces an eccentricity by Equation (19).

$$e = \frac{W_t \frac{B_h + W_s}{2} + S_{ah,1} \frac{H}{3} + S_{ah,2} \frac{H_w + D_F}{3} - W_h \frac{B_t - W_s}{2} - S_{av}\left(\frac{B_h + B_t - W_s}{2}\right)}{W_t + W_h + S_{av} - S_{pv} - U} + \frac{-S_w\left(\frac{H_w + D_F}{3}\right) - U\frac{W_s}{2}}{W_t + W_h + S_{av} - S_{pv} - U} \quad (19)$$

The total bearing force Q_{lim} is the sum of effective bearing force and buoyancy force, given by:

$$Q_{lim} = \left[q'_{lim} + \gamma_w (D_F + H_w)\right] B' L \quad (20)$$

2.4 Other actions and resisting mechanisms

The soil-foundation interface is subjected to resultant action forces, including a driving shear force *T*, which is the sum of horizontal earth pressures and horizontal water pressure, and a vertical resultant force *N*, which is the sum of the soil weight (adjusted for buoyancy) and vertical passive pressure. They are expressed as:

$$T = S_{ah} - S_{ph} - S_w \quad (21)$$

$$N = W_t + W_h + S_{av} - S_{pv} - U \quad (22)$$

For Peer Review

The force applied to the toe W_t consists of the weight of the soil and of the water above it, influenced by scour actions. The force on the heel W_h represents the weight of the retained soil and water, remaining unaffected by scour. These forces are expressed as follows:

$$W_t = B_t[D'_F\gamma + (H_w + D_F - D'_F)\gamma_w] \tag{23}$$

$$W_h = B_h\gamma H \tag{24}$$

where γ denotes the equivalent soil unit weight, which is the total weight of the saturated and unsaturated soil divided by the relevant overall soil volume.

The stem, i.e., the vertical structural element that directly retains the soil, is subject to the water thrust on the toe side S_w, which increases as the soil layer diminishes and the scour progresses, whose expression is:

$$S_w = \frac{1}{2}\gamma_w(H_w + D_F - D'_F)^2 \tag{25}$$

The wall-soil system is subject to the buoyancy force U, which is unaffected by scour and is given by:

$$U = (H_w + D_F)\,(B_t + B_h)\gamma_w \tag{26}$$

3. Limit-state functions

Three different limit-state functions are formulated to describe the failure mechanisms, namely geotechnical failure, overturning failure, and sliding failure. Geotechnical failure occurs if the vertical surcharge N exceeds the bearing capacity Q_{lim}, which corresponds to the bearing capacity factor f_{bc} defined below exceeding 1:

For Peer Review

$$f_{bc} = \frac{W_t + W_h + S_{av} - S_{pv}}{Q_{lim}} \quad (27)$$

Overturning failure occurs when the destabilising moments exceeding the stabilising moments, i.e. when the overturning factor defined in equation (28) exceeds 1. When the foundation is not undermined, overturning is measured at the edge of the foundation on the waterside. When scour undermines the foundation, the overturning of the retaining wall is measured at the point O of Figure 2b. As scour progresses, this point moves past the centre of the toe, foundation, and heel, and stabilizing forces become destabilizing. To account for this, various expressions of the overturning factor need to be considered; these are detailed in Appendix 2.

$$f_{ov} = \frac{M_{de}}{M_{st}} \quad (28)$$

Where M_{st} and M_{un} denote respectively the stabilising and destabilising moments.

Sliding failure occurs when driving sliding force T exceeds the sliding resistance T_{lim}, which corresponds to the sliding factor f_{sl} defined below exceeding 1.

$$f_{sl} = \frac{S_{ah} - S_{ph} - S_w}{(W_t + W_h + S_{av} - S_{pv} - U)\tan\phi'} \quad (29)$$

4. Strength reduction method

The stability of retaining walls at any given scour D_T can be evaluated using the three failure mechanisms described above, each based on its respective limit state function. The factor of safety for each of these mechanisms is assessed via the Strength Reduction Method (SRM) (EN 1997). The partial safety factor $\gamma_{\phi'}$ represents the reduction factor of the shearing

For Peer Review

resistance required to bring the soil to the onset of collapse. The factor of safety is quantified the ratio between the tangent of the actual friction angle, $\tan\phi'$, and the tangent of the friction angle associated with the onset of failure, $\tan\phi'_{crit}$.

$$\gamma_{\phi'} = \frac{\tan\phi'}{\tan\phi'_{crit}} \tag{30}$$

Let us consider the case of a retaining wall initially stable. To cause the retaining wall to fail, the $\tan\phi'$ needs to be decreased to a critical value $\tan\phi'_{crit}$ until collapse occurs. The reduction in soil friction angle affects both the demand and capacity in all failure mechanisms; it increases the active thrust and reduces the passive thrust respectively, thereby increasing the risk of sliding and overturning. At the same time, the lower friction angle underneath the foundation decreases the bearing capacity Q'_{lim} and decreases the sliding resistance T_{lim}, thus increasing the likelihood of failure by exceedance of bearing capacity and sliding.

Figure 3 shows an example of the resistance-to-action ratio for the three failure mechanisms against the reduction factor. As the reduction factor increases, soil friction angle reduces, and the resistance-to-action ratio also reduces. The intersection points between the resistance-to-action curve and the horizontal red line, where resistance-to-action equals 1, identify the partial safety factor for the individual mechanisms. The partial safety factor $\gamma_{\phi'}$ for the retaining wall is the minimum partial safety factors between the three mechanisms (the bearing capacity in the example shown in Figure 3). This corresponds to considering the system reliability as a series system, similarly to Daryani and Mohamad (2014).

For Peer Review

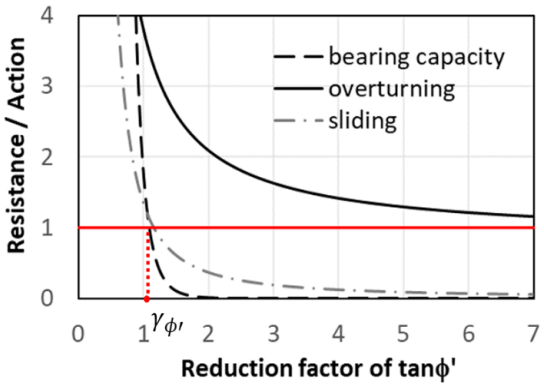

Figure 3. Resistance-to-action ratio and the reduction factor of $\tan\phi'$. Example of a retaining wall with the geometry of H=4.05 m, D_T=0, B_h=1.2 m, B_t=1.3 m, $D_F = H_w = \gamma_w = \delta = 0$, $\phi' = 28°$.

5. Model validation

The proposed closed-form solution is validated against numerical modelling using three structures representative of retaining walls in the UK road transport network. For each case study, the curve describing the reduction in the safety factor with increasing scour levels, derived from the section 2-4, is compared with the corresponding curve obtained using PLAXIS (PLAXIS 2020).

Figure 4 illustrates the transverse section of the walls and the corresponding simplified model used in the proposed formulation. The retaining wall in Figure 4a is modelled as a wall with no toe, whereas the one in Figure 4b as a wall with a toe and a heel. The retaining wall in Figure 4c is a typical cantilever wall with an inverted 'T' shape, which mostly utilize the weight of the backfill soil to provide the resistance to failure.

For Peer Review

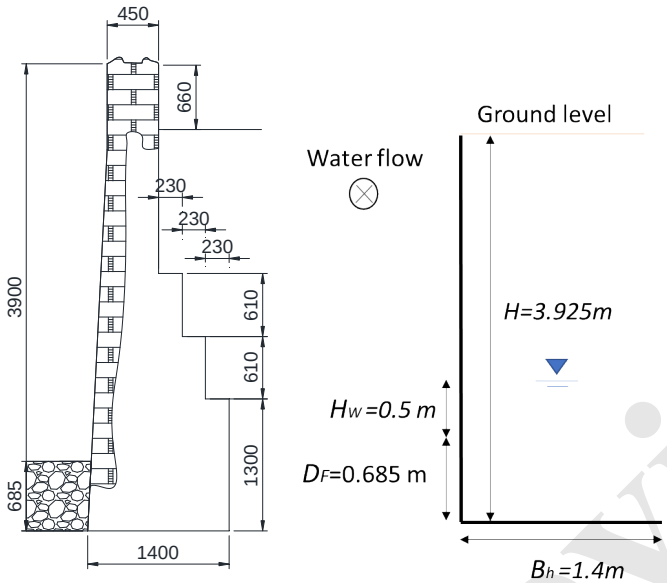

(a)

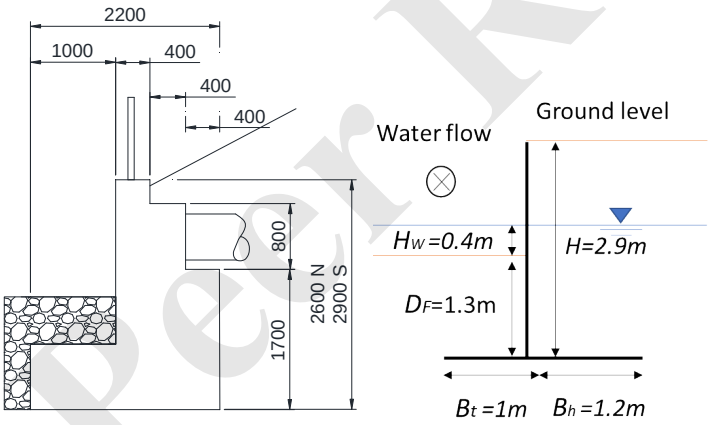

(b)

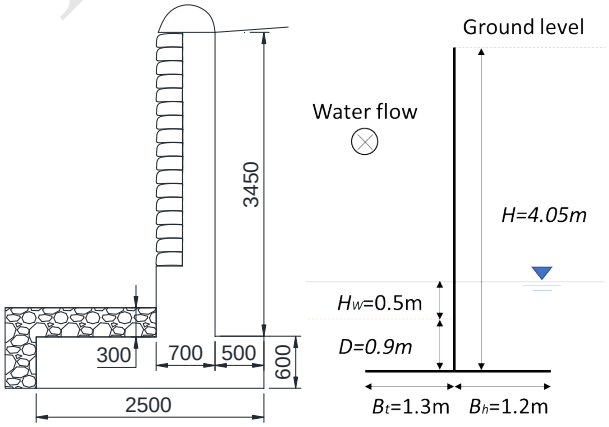

(c)

For Peer Review

Figure 4 Section drawings of retaining walls adjacent to the riverbank and their equivalent geometry in the closed-form solution. (a) retaining wall 1 (RW1) (b) retaining wall 2 (RW2) (c) retaining wall 3 (RW3)

Numerical models of the selected case studies, developed in PLAXIS 3D Version 20.03 (PLAXIS 2020), are used to calculate the variation of the factor of safety with increasing scour levels. To eliminate the impact of the boundaries on the results, the soil domain's height and width are set to be 8 times and 10 times the height of the wall, respectively. The ground has the displacement constrained in the out-of-plane direction to simulate a plane strain state. The mesh is refined into three zones, becoming progressively finer near the wall to enhance the accuracy of capturing soil deformation in its vicinity. The backfill and foundation soil are modelled with a homogeneous elasto-plastic material model with the failure surface described by the Mohr–Coulomb criterion, defined by the parameters Young's modulus $E_{ref}^{'}$ (kN/m^2), Poisson's ratio v, friction angle ϕ'(°), Dilatancy angle ψ' (°), Cohesion c' (kPa). It is noteworthy that the value of the friction angle of 20° used for the analysis of RW2 is rather low and has been considered here purely as an illustrative example, representing loose alluvial soils from riverbed material with low strength and bearing capacity. The retaining wall is represented by an elastic material with Young's moduli representing concrete with a compressive strength of 25 MPa (ACI 2011). Between the soil and the wall, interface elements are introduced. The stiffness and strength properties of the interfaces are derived from those of the surrounding soil. Table 1 illustrates the values adopted for the parameters of the three models.

Table 1. Values of parameters of PLAXIS models

Soil properties						Wall Properties		
Young's modulus $E_{ref}^{'}$ (kN/m^2)	Poisson's ratio v	Friction angle ϕ' (°)	Dilatancy angle ψ' (°)	Cohesion c' (kPa)	Bulk density γ (kN/m^3)	Young's modulus $E_{ref}^{'}$ (kN/m^2)	Poisson's ratio v	Density (kN/m^3)

For Peer Review

25700	0.286	RW1: 35 RW2: 20 RW3: 28	RW1: 35 RW2: 20 RW3: 28	0	20	23500000	0.15	25

Each case study was analysed in PLAXIS using a three-stage construction procedure. In the first stage, the retaining wall and the initial ground conditions were activated and brought to equilibrium. In the second stage, the scour process was simulated by progressively removing soil elements around the wall until a new equilibrium state was achieved. In the final stage, a strength-reduction analysis was performed, in which the shear strength parameters ϕ' and c were systematically reduced to identify the onset of global failure of the retaining wall system.

Figure 5 to Figure 7 illustrate the contour plot of the incremental deviatoric strains ε_q at the final step of the analysis for the selected case studies, under conditions of no scour and varying scour levels. The patterns of incremental deviatoric strains are similar at point A (no scour) and point B (scour depth equal to embedment depth). In both situations, failure planes develop across the backfill soil and extend below the foundation and towards the riverbed. When the foundation is undermined by scour (point C), the failure surfaces are still located below the foundation and within the backfill soil, but the affected area is smaller than in previous stages, suggesting a localisation of deformations. As scour progresses further (point D), the deviatoric strains are concentrated primarily near the back of the wall, suggesting that the overturning mode becomes critical when the critical scour condition is approached.

Figure 5 to Figure 7 also show the curves describing the reduction of safety factor based on the closed-form solutions for sliding, overturning, and foundation bearing capacity limit state, and the curve derived from the numerical analysis. For $D_T < D_F$, the sliding failure is the critical failure mechanism in RW2 and RW3. However, as scour progresses ($D_T \geq D_F$), the

For Peer Review

foundation bearing capacity limit state is characterised by the lowest safety factor and controls the failure. It is also worth observing that the curves for the overturning and bearing capacity limit state tend to converge to the same point at zero capacity. According to the proposed formulation, this point corresponds to the location of the resultant of the vertical loads. If the horizontal penetration of scour progresses beyond this point, equilibrium is not possible. This observation has important implications for the definition of a simplified expression for the reduction of safety of retaining walls due to scour in Section 2-4.

In general, it is interesting to observe that for low levels of scour, the safety factor reduces almost linearly for increasing scour levels, whereas for high levels of scour, a nonlinear, more significant reduction is observed until the critical condition of zero capacity is attained. Despite its underlying simplifying assumptions, the proposed formulation provides results quite close to the numerical results. The discrepancy between the results can be attributed mainly to the assumption of independent failure mechanisms and the fact that the bearing capacity is calculated using a semi-empirical approach to account for the eccentricity of the vertical force.

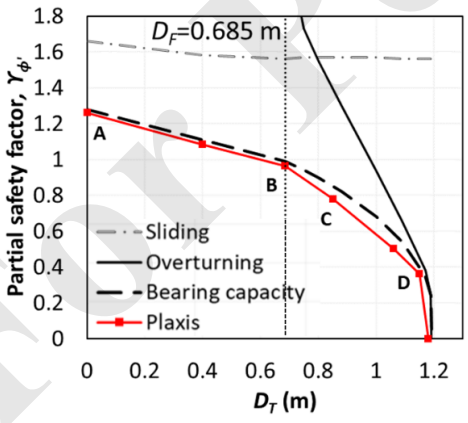

(a)

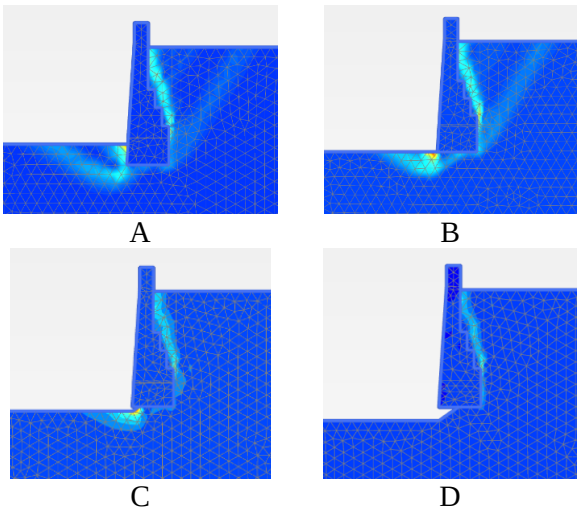

(b)

For Peer Review

Figure 5 Partial safety factor under scour for RW1 (a)closed-form solution and PLAXIS (b) incremental deviatoric strains contours show failure planes.

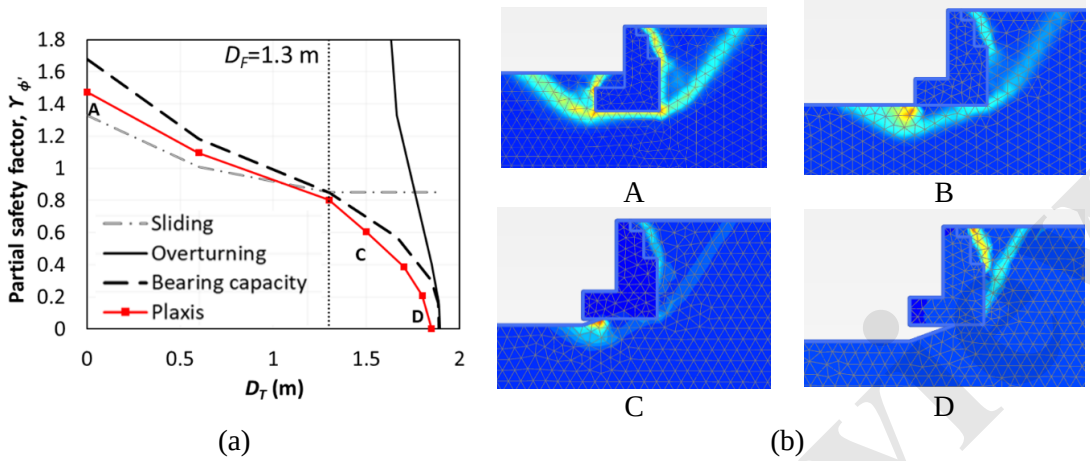

Figure 6 Partial safety factor under scour for RW2 (a)closed-form solution and PLAXIS (b) incremental deviatoric strains contours show failure planes.

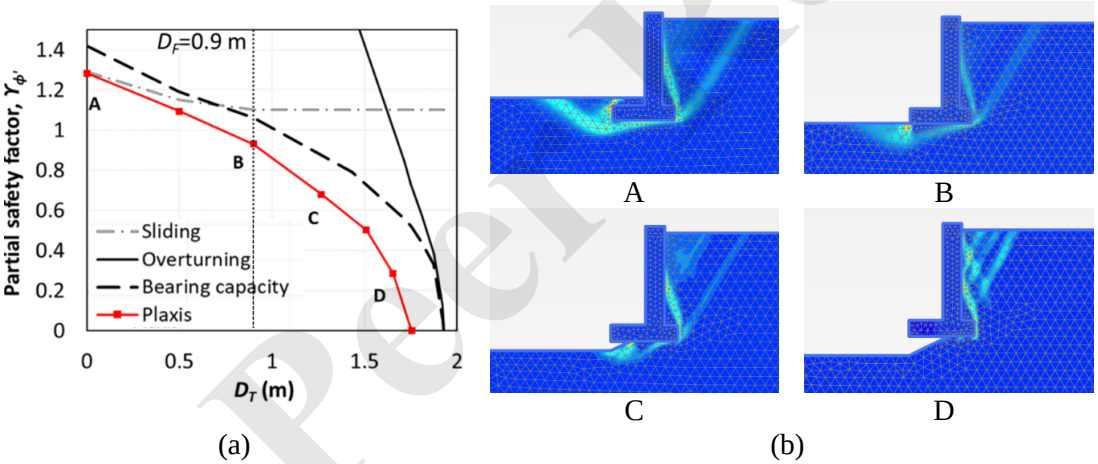

Figure 7 Partial safety factor under scour for RW3 (a) closed-form solution and PLAXIS (b) incremental deviatoric strains contours show failure planes.

6. Non-dimensional formulation

The partial safety factor for retaining walls subjected to scour is affected by several geometrical and mechanical parameters, including the wall height H, width of base B, width of toe B_t, embedded depth D_F, water depth H_w+D_F, friction angle of the base soil and retained soil ϕ', unit weight of the base soil and retained soil γ. In order to reduce the number of independent variables and highlight the most influential ones that control the problem, a

For Peer Review

dimensional analysis, using Buckingham's Pi theorem (Buckingham, 1914), is carried out. This approach is useful in parametric studies investigating various scenarios, by also preserving the relationships between parameters in a manner consistent with practical design principles. For instance, in the design of cantilever walls, the height-to-base width ratio typically falls within the range of 1 to 2. Table 2 illustrates the identified non-dimensional parameters and their range of variation, representing typical retaining wall designs in engineering practice (Sarıbaş and Erbatur 1996, Uray, Çarbaş et al. 2020, Kaveh, Biabani Hamedani et al. 2021). Table 2 illustrates the identified non-dimensional parameters and their range of variation, representing typical retaining wall designs in engineering practice (Sarıbaş and Erbatur 1996, Uray, Çarbaş et al. 2020, Kaveh, Biabani Hamedani et al. 2021). Regarding the water level, $(H_w+D_F)/H$ is assumed to vary between 0 and 0.6, where H_w+D_F represents the portion of the retaining wall below the water level. Accordingly, the relative footing depth D_F/H is assumed to fall within the range 0 to 0.3, and the normalized water depth H_w/H is likewise taken to vary between 0 and 0.3. It should be noted that higher relative water levels than those investigated may occur during extreme events leading to scour. However, considering a wider range of variation for H_w has no impact on the observed results.

Table 2 Non-dimensional in parameters controlling the problem and range of values.

Non-dimensional parameters		Symbol	Lower bound	Upper bound
Influencing parameters				
Π_1	Embedded depth of the wall//Height of the wall	D_F/H	0	0.3
Π_2	Width of the toe/width of the wall base	B_t/B	0	0.5
Π_3	Height of the wall /width of the wall base	H/B	1	2
Π_4	Friction angle of the base soil and retained soil	ϕ'	0.38	0.7
Π_5	Unit weight of the soil /Unit weight of water	γ/γ_w	1.6	2.8

For Peer Review

Π_6	Water level to foundation base level/Height of the wall	H_w/H	0	0.3
Π_7	Normalised scour demand	$D_T/D_{T,lim}$	0	1
Influenced variable				
	Partial factor under scour /partial factor at zero scour	$\gamma_{\phi'}/\gamma_{\phi'_0}$	0	1

To account for retaining walls characterized by a frictional behaviour at the wall-soil interface ($\delta > 0$), the interface friction angle is assumed equal to the soil's internal friction angle ($\delta = \phi'$). Moreover, to define the scour demand, the limit value of the scour depth is introduced, D_{Tlim}, defined as follows:

$$D_{Tlim} = D_F + (B_t + B_h/2) \cdot tan\phi' \quad (31)$$

The value of D_{Tlim} represents the condition where the foundation is undermined up to the centre of the heel. At this stage, the remaining soil beneath the heel cannot resist vertical gravitational forces corresponding to the retained soil, and thus stability is not possible regardless of the value of ϕ' , i.e., $\frac{\gamma_{\phi'}}{\gamma_{\phi'_0}} = 0$. The results obtained for the previously analysed case studies confirm this. The value of D_{Tlim} for RW1, RW2, and RW3 is 1.9 m, 1.9 m, and 1.2 m, respectively, which corresponds to the points where $\gamma_{\phi'}$=0 in Figure 5a, Figure 6a, and Figure 7a. As will be shown below, the proposed non-dimensional scour measure enables the identification of a single master curve, providing a unified, scaled representation onto which all data points, regardless of material or conditions.

In order to evaluate the influence of the non-dimensional parameters on the safety of retaining walls for different levels of scour, $N_{samples}$=6380 combinations of the non-dimensional parameters are generated, assuming uniform distributions between their respective lower and upper bounds. For each sample combination, corresponding to a wall-soil-water configuration, the normalised partial safety factor $\frac{\gamma_{\phi'}}{\gamma_{\phi'_0}}$ is determined for increasing values of the dimensionless scour depth $\frac{D_T}{D_{Tlim}}$ in the range from 0 to 1. The relationship

For Peer Review

between $\frac{\gamma_{\phi'}}{\gamma_{\phi'_0}}$ and $\frac{D_T}{D_{Tlim}}$ is then plotted, considering the combined effects of the multiple variables. Figure 8 illustrates the result of the analysis for the case of D_F/H=0 and D_F/H≥0. Despite significant variations in wall geometry, water depth, and soil properties, the reduction in the safety factor collapses onto a single master curve (red curve in Figure 8a). Notably, in the case of D_F/H=0 (a), the data exhibit minimal scatter from the master curve, which means that the reduction of the normalised partial factor is governed solely by the normalised scour depth and is independent of other non-dimensional parameters. The master curve can be approximated by Equation (32):

$$\frac{\gamma_{\phi'}}{\gamma_{\phi'_0}} = (1 - \frac{D_T}{D_{Tlim}})^{0.4} \quad (32)$$

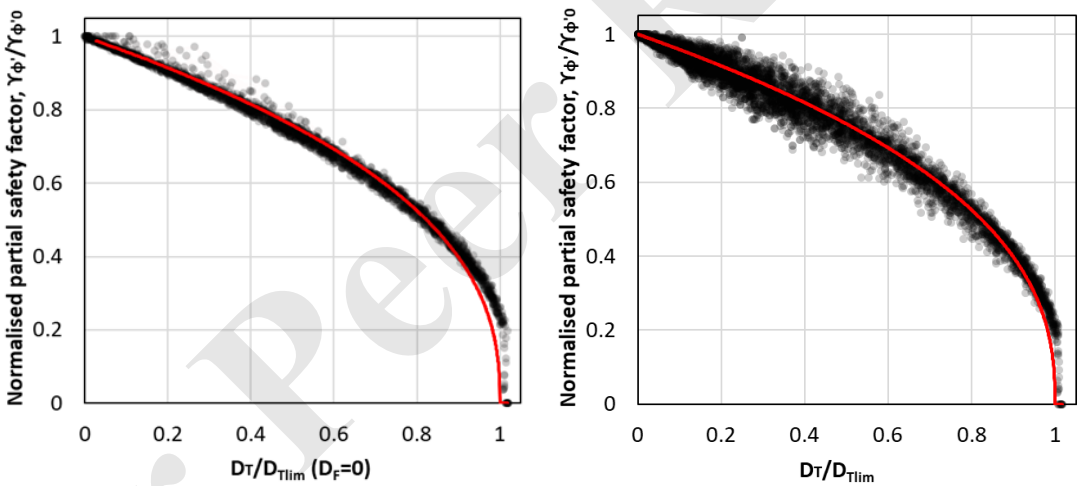

Figure 8 The reduction of partial safety factor under progressive scour $\frac{D_T}{D_{Tlim}}$ for (a) D_F/H=0 (b) D_F/H≥0.

When D_F/H≥0 (Figure 8b), the variance of the data points and the scatter from the master curve increase. To investigate the source of variance under different levels of scour, global sensitivity analysis (Sobol 2001) is carried out to quantify the contribution of each variable and their interaction to the variance of the model output $\frac{\gamma_{\phi'}}{\gamma_{\phi'_0}}$. The sensitivity analysis is

For Peer Review

carried out at fixed values of the normalised scour depth, corresponding to values of $\frac{D_T}{D_{Tlim}}$ of 0.15, 0.3, 0.45, 0.6, 0.75, 0.9. At each scour level, the total output variance $V(\frac{\gamma_{\phi'}}{\gamma_{\phi'_0}})$ is evaluated by the variance of the expected value of $\frac{\gamma_{\phi'}}{\gamma_{\phi'_0}}$ conditioned on a fixed value of Π_i. The second-order effect, V_{ij}, is the joint effect of Π_i and Π_j minus the first-order effects for the same factor. The contribution of each input on the output variability is represented by Sobol indexes. The first-order Sobol index S_i quantifies the effect of input Π_i, while the total Sobol index S_{T_i} includes first-order effects of input Π_i plus all higher-order effects due to interaction.

The sensitivity analysis is conducted using the SobolGSA toolbox (Kucherenko 2013). The nondimensional factors are treated as independent random variables with uniform distributions over their respective ranges.

Figure 9 presents the sensitivity indices of Π_1,Π_2,...,Π_6 under different levels of scour. In general, it can be observed that these indices vary significantly with scour. In the early scour stage ($\frac{D_T}{D_{Tlim}}$< 0.15), D_F/H and H_w/H govern the output uncertainty, then their contribution gradually reduces. The total index for D_F/H stays above 0.2, while that for H_w/H drops to a negligible value after $\frac{D_T}{D_{Tlim}}$=0.3. In contrast, the indices for B_t/B, H/B, and ϕ' increase with scour and play secondary roles. The total sensitivity index of B_t/B rises from 0 to 0.3, then remains nearly flat with a slight decline to a value of 0.2. Meanwhile, the total sensitivity index of H/B consistently increases from 0 to 0.35 until $\frac{D_T}{D_{Tlim}}$=0.75. The increasing impact of H/B suggests the involvement of overturning failure, as higher H/B increases active pressure and the risk of overturning under the same scour conditions. The total sensitivity index of ϕ' increases from zero at the unscoured condition, peaks at 0.45, then decreases to 0.2, showing a hump trend. This reflects that ϕ' has double effects on the stability of retaining walls; a

For Peer Review

higher value of ϕ' increases the stability of the wall-soil system, but it can make it more unstable by steepening the inclination of the scour hole under the wall base. Compared with other variables, γ/γ_w has a negligible impact on the results and remains flat throughout.

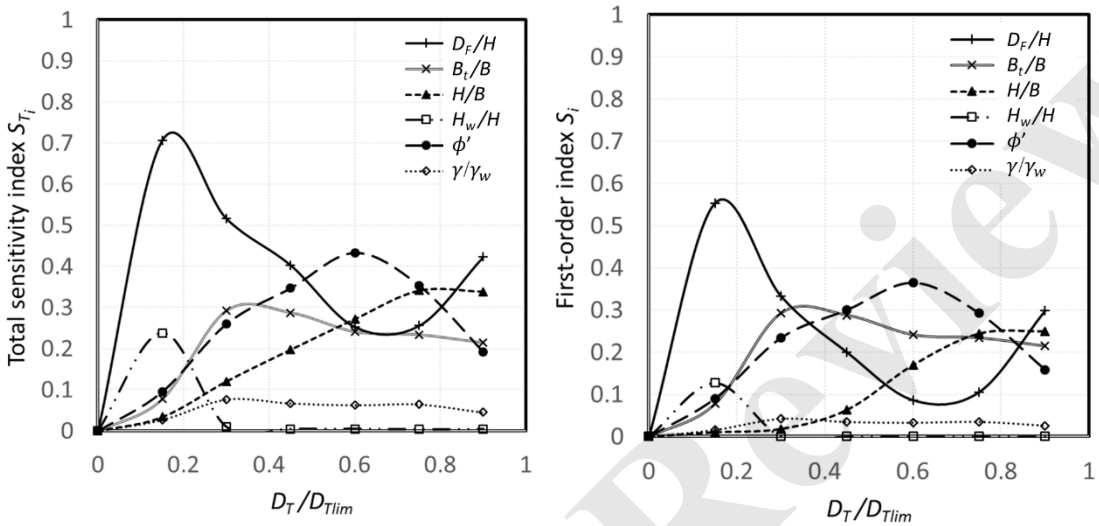

Figure 9 Sensitivity indices of non-dimensional variables under fix value of scour: (a) total sensitivity indices (b) first-order indices

The main outcome of the global sensitivity analysis is that many non-dimensional parameters have an impact on the output variance, and this impact changes with the scour depth. Thus, it is unpractical to attempt to derive an expression more sophisticated than Equation (32) to explicitly describe the effect of each parameter on the reduction of the safety factor. Rather than doing this, it is preferable to keep Equation (32) to estimate $\frac{\gamma_{\phi'}}{\gamma_{\phi'_0}}$ and derive a simple expression for quantifying its uncertainty. For this purpose, the relative squared errors (ε_i^2, i=1, 2,.., $N_{samples}$) and coefficient of variation (cov_s) are evaluated for increasing values of the normalized scour. We remind the reader that the relative squared error ε_i^2 of the i-th sample is defined as the square of the difference between the fitted values implied by equation (32) and the true value from the closed-form solution, divided by the true value. Figure 10 plots the relative squared errors ε_i^2 of the samples as a function of $\frac{D_T}{D_{Tlim}}$ and an estimate of cov_s^2

For Peer Review

obtained using a moving average method. It can be observed that the uncertainty cov_s^2 is zero when the scour is zero, increases progressively with scour until $\frac{D_T}{D_{Tlim}} = 0.5$, after which it is effectively constant. Based on this observation, a simplified expression can be derived for cov_s^2:

$$\mathrm{cov}_s^2 = min\left(0.06\frac{D_T}{D_{Tlim}}, 0.003\right) \quad (33)$$

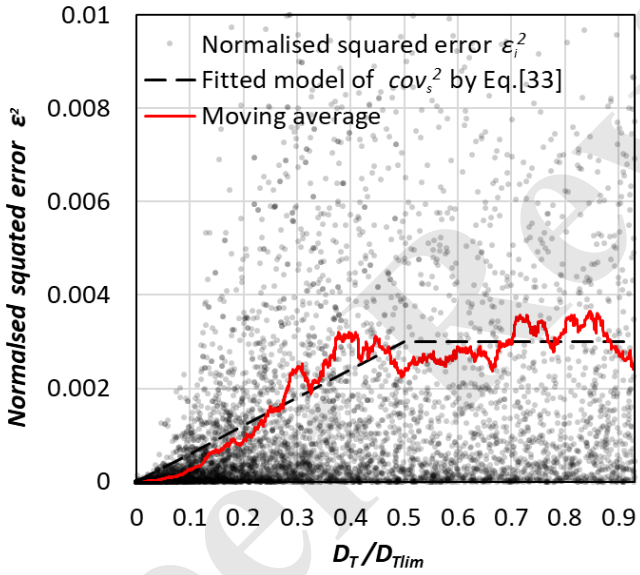

Figure 10 Variation of normalised squared error $\boldsymbol{\varepsilon^2}$ and $\mathbf{cov}_s^2$ with increasing scour.

7. Scour vulnerability model

In this section, a simplified model is derived for the scour vulnerability of retaining walls, based on reliability-based principles. This model links the probability of failure conditional to the scour level, by exploiting the closed-form expressions derived in the previous section for the mean reduction of the normalised safety factor due to scour and its coefficient of variation.

The safety factor $\gamma_{\phi'}$ of the retaining wall associated with the most critical failure mode is an uncertain quantity, whose variability depends on the design uncertainties and the additional uncertainty in capacity brought by scour. Assuming that $\gamma_{\phi'}$ is a random variable with

For Peer Review

lognormal distribution, mean value $E(\gamma_{\phi'})$ and coefficient of variation cov_Z, the probability of failure of the retaining wall can be expressed as:

$$P_F = \Phi(-\beta) \tag{34}$$

where Φ is the cumulative standard normal distribution and β is the Rosenblueth's and Esteva's reliability index (Rosenblueth and Esteva 1972), expressed by :

$$\beta = \frac{ln\, E(\gamma_{\phi'})}{cov_Z} \tag{35}$$

The uncertainty of the safety factor cov_Z combines the design uncertainty cov_0 and the additional uncertainty introduced by scour cov_s according to:

$$cov_Z = \sqrt{cov_0^2 + cov_s^2} \tag{36}$$

where uncertainty cov_s is quantified by equation (33), and the design uncertainty cov_0 is evaluated by a retaining wall with no scour. Similar to the general case, reliability index β_0 depends on the mean value of the design safety factor $E(\gamma_{\phi'_0})$ and the design uncertainty cov_0 through Rosenblueth's and Esteva's formula:

$$\beta_0 = \frac{E(\gamma_{\phi'_0})}{cov_0} \tag{37}$$

The design reliability β_0 depends on the level of overdesign of the retaining wall. It should be noted that the target failure probabilities of retaining walls are still very much unknown (He, Fenton and Griffiths 2022). According to Eurocode guidelines, a target reliability index β_0 of 3.8 is considered acceptable for designing retaining walls type structures under ultimate limit states (EN 1990:2002), and a nominal partial factor $\gamma_{\phi'_0}$ of 1.25 is recommended for the soil friction angle to have adequate safety margins in design under ultimate limit states (EN 1997). Assuming that the retaining walls was properly designed in compliance with the Eurocode requirements, with no overdesign, the design coefficient of variation cov_0 can be estimated as:

For Peer Review

$$cov_0 = \frac{ln\,\gamma_{\phi'_0}}{\beta_0} = \frac{ln\,1.25}{3.8} \approx 6\% \tag{38}$$

Respect to the design situation, scour reduces the reliability of the retaining wall as it reduces the wall's mean safety factor (as per equation (32)) and increases its uncertainty (as per equation (33)). It is convenient to rearrange equation (37) to highlight the contribution of the design reliability β_0. In formula:

$$\beta = \frac{ln\,E(\gamma_{\phi'})}{cov_Z} = \frac{\frac{ln\,E(\gamma_{\phi'_0})}{cov_0}\,cov_0 + ln\frac{E(\gamma_{\phi'})}{E(\gamma_{\phi'_0})}}{cov_Z} = \frac{\beta_0 \cdot cov_0 + ln\,E\left(\frac{\gamma_{\phi'}}{\gamma_{\phi'_0}}\right)}{\sqrt{cov_0^2 + cov_s^2}} \tag{39}$$

where we have accepted the approximation:

$$\frac{E(\gamma_{\phi'})}{E(\gamma_{\phi'_0})} \cong E\left(\frac{\gamma_{\phi'}}{\gamma_{\phi'_0}}\right) \tag{40}$$

The loss in reliability $\Delta\beta$ caused by scour can also be expressed in closed form by:

$$\Delta\beta = \beta - \beta_0 = \beta_0\left(\frac{cov_0}{\sqrt{cov_0^2 + cov_s^2}} - 1\right) + \frac{ln\,E\left(\frac{\gamma_{\phi'}}{\gamma_{\phi'_0}}\right)}{\sqrt{cov_0^2 + cov_s^2}} \tag{41}$$

Equation (39), together with (34), effectively provides an expression for the retaining wall's vulnerability as a function of the normalized scour depth $\frac{D_T}{D_{Tlim}}$:

$$P_F = \Phi(-\beta) = \Phi\left(-\frac{\beta_0 \cdot cov_0 + ln\,E\left(\frac{\gamma_{\phi'}}{\gamma_{\phi'_0}}\right)}{\sqrt{cov_0^2 + cov_s^2}}\right) \tag{42}$$

Equation (42) indicates that the scour vulnerability of retaining walls depends on four factors:

- the design reliability β_0 generally provided by (37) or conservatively assumed equal to 3.8;
- the design uncertainty cov_0 which can be assumed equal to 6% as per (38);
- the expected loss in safety factor $E\left(\frac{\gamma_{\phi'}}{\gamma_{\phi'_0}}\right)$ due to scour, quantified by (32);
- the additional uncertainty cov_s introduced by scour, quantified by (33)

For Peer Review

To illustrate the simplicity and practical effectiveness of the method, the vulnerability curves are derived for the three retaining walls with varying geometries shown in Figure 4. Table 3 lists the values of the wall and soil parameters needed to estimate D_{Tlim} which include the toe width, heel width, and embedded depth, extracted from the section drawing of the retaining walls, as well as the soil friction angle representative of the riverbed material, which is assumed. The value of β_0 can be assumed equal to 3.8 without performing any analysis of the retaining wall, based on the assumption that the wall satisfies the minimum reliability requirements. Alternatively, a more accurate β_0 can be estimated by the nominal partial safety factor $\gamma_{\phi'_0}$ in the case of no scour, which is evaluated by using the proposed closed-form method, together with cov_0 in equation (38) .

Table 3 Input parameters for estimating the probability of failure of retaining walls under scour

Case studies	Embedded depth D_F (m)	Soil friction angle ϕ' (°)	Toe width B_t (m)	Heel width B_h (m)	$\gamma_{\phi'_0}$	β_0
RW1	0.685	35	0	1.4	1.28	3.9
RW2	1.3	20	1	1.3	1.33	4.8
RW3	0.9	28	1.3	1.2	1.29	4.2

Figure 11 shows the vulnerability curves obtained for the selected case studies, conditional to the level of scour, as described by D_T or $\frac{D_T}{D_{Tlim}}$, in both the linear and semi-logarithmic scale. The curves in Figure 11a have been derived considering the values of β_0 reported in Table 3, corresponding to the actual values of $\gamma_{\phi'_0}$. The baseline vulnerability curve obtained for the Eurocode's target reliability β_0 = 3.8 is also plotted in the same figures, as dashed curves, for comparison. As expected, the probability of failure increases with scour and differs for the various walls. When the scour depth is expressed in dimensionless form, the vulnerability

For Peer Review

curves are closer to each other, and they differ only due to their different design reliability β_0, i.e. due to their different overdesign. Therefore, the baseline vulnerability curves, which have the same β_0 = 3.8, coincides in Figure 11b and represented by the red dashed curve (i.e., the Ref. curve).

The vulnerability curves on a logarithmic scale highlight the impact of scour on the probability of failure across several orders of magnitude (Figure 11c and Figure 11d). At zero scour depth, each retaining wall starts from a different value of probability of failure, with RW2 having the lowest value (1e^{-6}) and the reference case the highest value (7.5e^{-5}). The failure probability rises sharply by several orders of magnitude due to scour: in the reference case, the failure probability increases by one, two, and three orders of magnitude for values of the normalised scour level of 0.07, 0.15, and 0.28. It is also worth to observe that the failure probability reaches the value of 1 when $\frac{D_T}{D_{Tlim}}$ approaches 0.7, regardless of the initial value of β_0. Use of the reference curve is recommended in absence of more detailed information on the overdesign level, since it provides conservative estimates of the vulnerability.

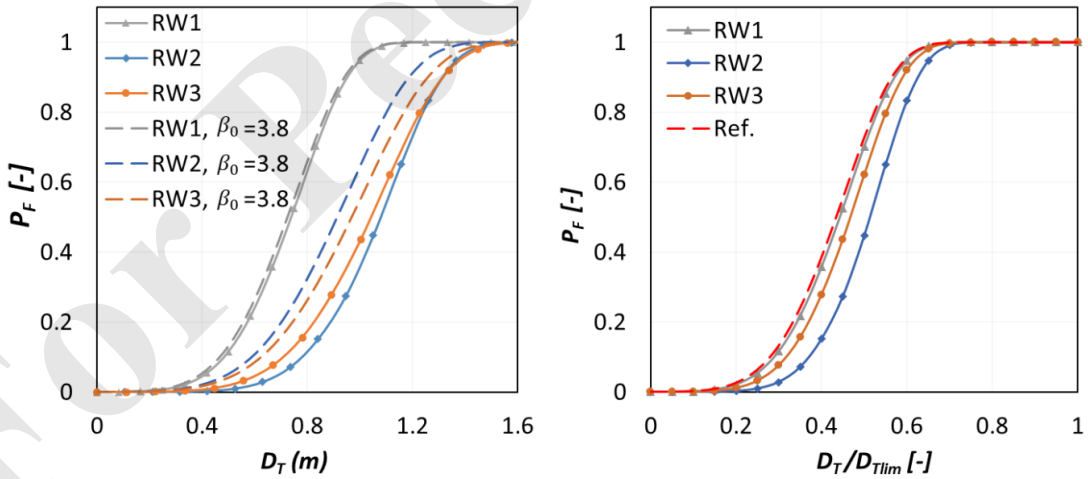

(a) (b)

For Peer Review

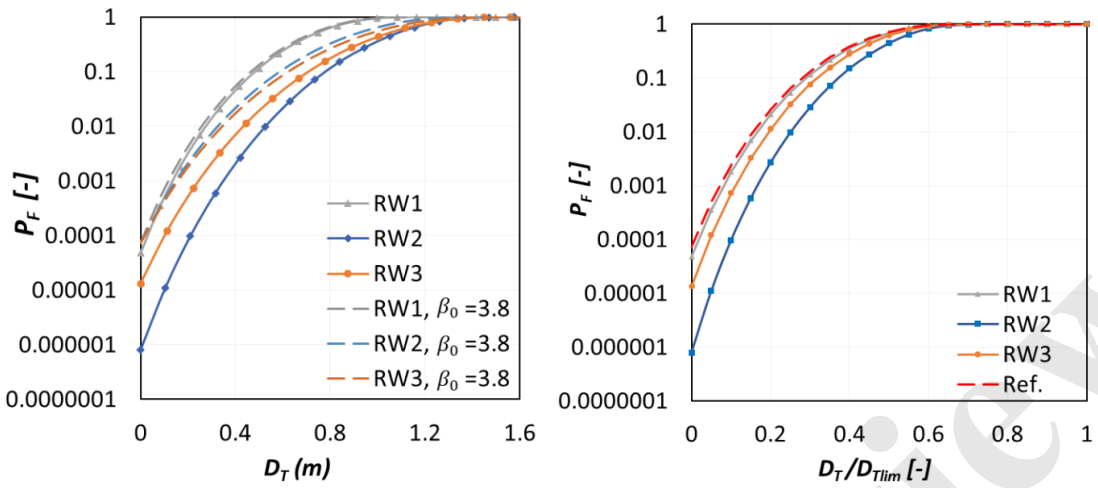

(c) (d)

Figure 11 Vulnerability curves of the retaining walls (a) dimensional scour presentation (b) non-dimensional scour presentation (c) dimensional scour on a logarithmic scale of P_F (d) non-dimensional scour on a logarithmic scale of P_F.

8. Conclusion

This study has introduced a novel, simplified analytical approach to evaluate the safety of retaining walls under scour conditions, effectively addressing a key gap in the assessment of their vulnerability. The analytical approach commonly used for the stability analysis of retaining walls has been extended in this study to account for the effects of scour on the most critical failure mechanisms—namely, overturning, sliding, and loss of base support. Closed-form expressions have been developed and validated against numerical modelling using three representative retaining walls in the UK transport network, showing good accuracy across a range of wall geometries, soil properties, and hydraulic conditions. Moreover, by expressing the problem in dimensionless terms and applying global sensitivity analysis, the study has proposed a nondimensional scour measure, which enables identification of a single master curve that provides a unified and scaled representation of the safety factor reduction, regardless of the variation in wall configurations, water depths, and riverbed and soil properties. Finally, a model for the scour vulnerability of retaining walls has been developed

For Peer Review

based on a reliability-based framework, by exploiting the closed-form expressions for the mean safety factor reduction and its coefficient of variation.

The proposed method enables rapid estimation of scour vulnerability of retaining walls using basic input parameters, making it suitable for infrastructure asset management and prioritizing maintenance and intervention strategies in flood-prone areas. Future work will extend this method to other retaining wall typologies (e.g. gabion walls, diaphragm walls and anchored walls) and will also provide practical guidelines for implementation in scour risk assessment and management procedures.

Acknowledgements: this financial support of National Highways through the project 'Foundations: improving risk assessment and prioritisation processes for management of scour at structures' is greatly acknowledged. This project is a collaboration with Connected Places Catapult, funded by the Engineering and Physical Sciences Research Council's Innovation Launchpad Network+ Researcher in Residence scheme (grant numbers EP/W037009/1, EP/X528493/1).

References

ACI (2011). Building Code Requirements for Structural Concrete (ACI 318-11), American Concrete Institute.

Argyroudis, S. A. and S. A. Mitoulis (2021). "Vulnerability of bridges to individual and multiple hazards- floods and earthquakes." Reliability Engineering & System Safety **210**: 107564.

Buckingham, E. (1914). "On physically similar systems; illustrations of the use of dimensional equations." Physical Review 4(4): 345–376.

Cely Calixto, N. J., A. Galvis Castaño and G. A. Carrillo Soto (2023). "Evaluation of Local Scour along the Base of Longitudinal Training Walls." Water 15(22): 4001.

Cerema (2019). Analyse de risque des ponts en site affouillable (in French). Collection: Références.

CIRIA (2015). Manual on scour at bridges and other hydraulic structures, second edition (C742).

CIRIA (2021). Manual on scour at bridges and other hydraulic structures - supplementary guide (SP171).

For Peer Review

Daryani, K. E., and Mohamad, H. (2014). System reliability-based analysis of cantilever retaining walls embedded in granular soils. *Georisk: Assessment and Management of Risk for Engineered Systems and Geohazards*, *8*(3), 192-201.

EN (1990:2002). Eurocode: Basis of structural design.

EN (1997). Eurocode 7 geotechnical design—part 1: general rules.

Fael, C. S., G. Simarro-Grande, J. P. Martín-Vide and A. H. Cardoso (2006). "Local scour at vertical-wall abutments under clear-water flow conditions." Water Resources Research **42**.

Hansen, J. B. (1970). "A revised and extended formula for bearing capacity."

He, P., G. A. Fenton, and D. V. Griffiths (2023). "Calibration of resistance factors for gravity retaining walls." Georisk: Assessment and Management of Risk for Engineered Systems and Geohazards, **17**(3): 586-594.

Heydari, N. and P. Diplas (2020). "Flow dynamics in the vicinity of a gravel embedded vertical retaining wall: conditions corresponding to the initial stages of local erosion." Environmental Fluid Mechanics **20**(1): 203-225.

Huang, C.-C. (2017). "Failure mechanisms of steep-faced geosynthetic-reinforced retaining walls subjected to toe scouring." Marine Georesources & Geotechnology **35**(8): 1099-1110.

Kaveh, A., K. Biabani Hamedani and A. Zaerreza (2021). "A set theoretical shuffled shepherd optimization algorithm for optimal design of cantilever retaining wall structures." Engineering with Computers **37**(4): 3265-3282.

Khosronejad, A., P. Diplas, D. Angelidis, Z. Zhang, N. Heydari and F. Sotiropoulos (2020). "Scour depth prediction at the base of longitudinal walls: a combined experimental, numerical, and field study." Environmental Fluid Mechanics **20**(2): 459-478.

Kucherenko, S. (2013). "SobolHDMR: a general-purpose modeling software." Methods Mol Biol **1073**: 191-224.

Lancellotta, R. (2002). "Analytical solution of passive earth pressure." Géotechnique **52**(8): 617-619.

McKelvey, J. A. III (2011). "Lessons learned from failures: The wall of shame." In Geo-Frontiers 2011: Advances in Geotechnical Engineering, 3235–3244.

NationalHighways (2024). CS 469 - Management of scour and other hydraulic actions at highway structures.

PLAXIS (2020). PLAXIS 3D Reference manual CONNECTION edition V20.03.

Rosenblueth, E. and L. Esteva (1972). Reliability Basis for Some Mexican Codes.

For Peer Review

Sarıbaş, A. and F. Erbatur (1996). "Optimization and sensitivity of retaining structures." Journal of Geotechnical Engineering **122**(8): 649-656.

Scozzese, F., E. Tubaldi and A. Dall'Asta (2023). "Damage metrics for masonry bridges under scour scenarios." Engineering Structures **296**: 116914.

Sobol, I. M. (2001). "Global sensitivity indices for nonlinear mathematical models and their Monte Carlo estimates." Mathematics and Computers in Simulation **55**(1): 271-280.

Sotiropoulos, F. and P. Diplas (2017). "Scour at the base of retaining walls and other longitudinal structures: Final report." NCHRP, Transportation Research Board, The National Academies.

Theinat, A. K., R. Salgado, M. Prezzi and V. A. Sakleshpur (2024). "Stability and factor of safety of gravity-retaining structures using the strength reduction method." J Journal of Geotechnical and Geoenvironmental Engineering.

Tubaldi, E., C. J. White, E. Patelli, S. A. Mitoulis, G. de Almeida, J. Brown, M. Cranston, M. Hardman, E. Koursari, R. Lamb, H. McDonald, R. Mathews, R. Newell, A. Pizarro, M. Roca and D. Zonta (2022). "Invited perspectives: Challenges and future directions in improving bridge flood resilience." Nat. Hazards Earth Syst. Sci. **22**(3): 795-812.

Uray, E., S. Çarbaş, İ. H. Erkan and M. Olgun (2020). "Investigation of optimal designs for concrete cantilever retaining walls in different soils." Challenge Journal of Concrete Research Letters; Vol 11, No 2 (2020)DO - 10.20528/cjcrl.2020.02.003.

Vesić, A. S. (1973). "Analysis of Ultimate Loads of Shallow Foundations." Journal of the Soil Mechanics and Foundations Division **99**(1): 45-73.

For Peer Review

Appendix 1: Earth pressures for cantilever walls adjacent to river and under scour actions

A1.1 Active thrust

Figure A-1 shows an ideal model of retaining wall and the location of active pressure, which is assumed to be applied at the edge of the heel.

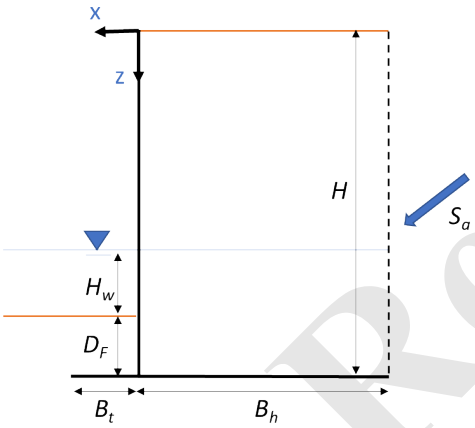

Figure A-1 Ideal model for active pressure of retaining wall adjacent to river

The horizontal and vertical components of active thrust are calculated by integrating the horizontal total stress σ_x and the tangential stress τ_{xz} respectively along the height H of the wall.

$$S_{ah} = \int_0^H (\sigma'_x + u_w)\, dz = \frac{1}{2} k_a \gamma H^2 + \frac{1}{2}(1 - k_a)\gamma_w (H_w + D_F)^2 \quad \text{(A1-1)}$$

$$S_{av} = \int_0^H \tau_{xz}\, dz = \int_0^H k_a^* \sigma'_z\, dz = \frac{1}{2} k_a^* \gamma H^2 - \frac{1}{2} k_a^* \gamma_w (H_w + D_F)^2 \quad \text{(A1-2)}$$

$$k_a = \frac{\cos\delta}{1 + \sin\phi'} \left(\cos\delta - \sqrt{\sin^2\phi' - \sin^2\delta}\right) e^{-2\theta \tan\phi'} \quad \text{(A1-3)}$$

For Peer Review

$$k_a^* = \tan\delta\, k_a \tag{A1-4}$$

$$2\theta = \operatorname{asin}\left(\frac{\sin\delta}{\sin\phi'}\right) - \delta \tag{A1-5}$$

$$u_w = \gamma_w\left[z - \left(H - (H_w + D_F)\right)\right] \tag{A1-6}$$

A1.2: Passive thrust

Figure A-2 shows the retaining wall and the location of passive pressure, which is assumed to be applied at the edge of the toe.

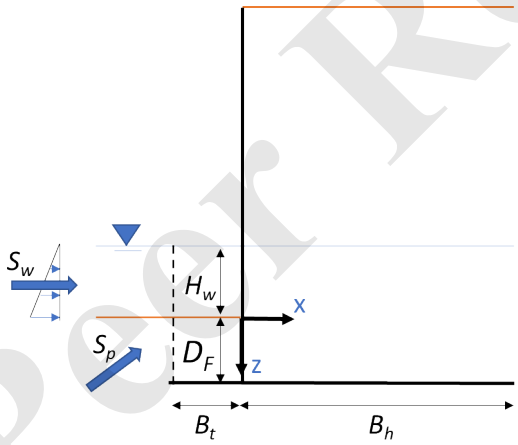

Figure A-2 Ideal model for passive pressure of retaining wall adjacent to river

The horizontal and vertical components of passive thrust are calculated by integrating the horizontal total stress σ_x and the tangential stress τ_{xz} respectively along t embedded depth and the height of water.

$$S_{ph} = \int_0^{D_F} \sigma_x\, dz = \frac{1}{2}(\gamma - \gamma_w)k_p{D_F}^2 + \left(\frac{1}{2}\gamma_w{D_F}^2 + \gamma_w H_w D_F\right) \tag{A1-7}$$

For Peer Review

$$S_{pv} = \int_0^{D_F} \tau_{xz}\, dz = \int_0^{D_F} k_p^*(\sigma_z - u_w)\, dz = \frac{1}{2}(\gamma - \gamma_w) k_p^* {D_F}^2 \quad \text{(A1-8)}$$

$$k_p = \frac{\cos\delta}{1 - \sin\phi'}\left(\cos\delta + \sqrt{\sin^2\phi' - \sin^2\delta}\right) e^{2\theta \tan\phi'} \quad \text{(A1-9)}$$

$$k_p^* = \tan\delta\, k_p \quad \text{(A1-10)}$$

$$2\theta = \operatorname{asin}\left(\frac{\sin\delta}{\sin\phi'}\right) + \delta \quad \text{(A1-11)}$$

$$u_w = \gamma_w(H_w + z) \quad \text{(A1-12)}$$

Appendix 2: Overturning failure of retaining wall under progressive scour

For $D_T \leq D_F$, the overturning point is at the edge of the toe on the water side, and the overturning factor given by:

$$f_{ov} = \frac{S_{ah,1}\frac{H}{3} + S_{ah,2}\frac{H_w + D_F}{3} + U\frac{B_t + B_h}{2}}{S_{av}(B_h + B_t) + W_h\left(\frac{B_h}{2} + B_t\right) + W_t\left(\frac{B_t}{2}\right) + S_w\left(\frac{H_w + D_T}{3} + D_F^{'}\right) + S_{ph,1}\frac{D_F^{'}}{3} + S_{ph,2}\frac{D_F^{'}}{2}} \quad \text{(A2-1)}$$

When $D_T > D_F$ and $0 < W_s \leq B_t/2$, the foundation is exposed, and the passive pressure is zero. The overturning point moves toward the heel but does not exceed the centre of the toe. This shift changes the overturning arm for active pressure, buoyancy force, and the vertical resultant forces on wall base. The expression of the overturning factor becomes:

For Peer Review

$$f_{ov} = \frac{S_{ah,1}\frac{H}{3} + S_{ah,2}\frac{H_w + D_F}{3} + U|W_s - \frac{B_t + B_h}{2}|}{S_{av}|B_h + B_t - W_s| + W_h|\frac{B_h}{2} + B_t - W_s| + W_t|\frac{B_t}{2} - W_s| + S_w\left(\frac{H_w + D_F}{3}\right)} \quad \text{(A2-2)}$$

When $D_T > D_F$ and $B_t/2 < W_s \leq B_t/2 + B_h/2$, the overturning point moves further toward the heel, causing W_t to act as a destabilising force. The overturning factor is:

$$f_{ov} = \frac{S_{ah,1}\frac{H}{3} + S_{ah,2}\frac{H_w + D_F}{3} + W_t|\frac{B_t}{2} - W_s| + U|W_s - \frac{B_t + B_h}{2}|}{S_{av}|B_h + B_t - W_s| + W_h|\frac{B_h}{2} + B_t - W_s| + S_w\left(\frac{H_w + D_F}{3}\right)} \quad \text{(A2-3)}$$

When $D_T > D_F$ and $(B_t + B_h)/2 \leq W_s < B_t + B_h/2$, the overturning point moves beyond the centre of the foundation, causing the buoyancy to act as a stabilization force. Thus, the overturning factor is given by:

$$f_{ov} = \frac{S_{ah,1}\frac{H}{3} + S_{ah,2}\frac{H_w + D_F}{3} + W_t|\frac{B_t}{2} - W_s|}{S_{av}|B_h + B_t - W_s| + W_h|\frac{B_h}{2} + B_t - W_s| + S_w\left(\frac{H_w + D_F}{3}\right) + U|W_s - \frac{B_t + B_h}{2}|} \quad \text{(A2-4)}$$

Finally, when $D_T > D_F$ and $W_s \geq B_t + B_h/2$, the overturning point moves beyond the centre of the heel, and W_h becomes a destabilizing force.

$$f_{ov} = \frac{S_{ah,1}\frac{H}{3} + S_{ah,2}\frac{H_w + D_F}{3} + W_t|\frac{B_t}{2} - W_s| + W_h|\frac{B_h}{2} + B_t - W_s|}{S_{av}|B_h + B_t - W_s| + S_w\left(\frac{H_w + D_F}{3}\right) + U|W_s - \frac{B_t + B_h}{2}|} \quad \text{(A2-5)}$$

For Peer Review

Response to Reviewer's comments

Title: **Vulnerability Model for Cantilever Retaining Walls Subject to Scour**

Authors: Lanting Wei, Alessandro Tarantino, Enrico Tubaldi*, Hamed Moghaddasi, and Daniele Zonta

Original manuscript ID: 259196278

The authors gratefully acknowledge the constructive criticism of the Reviewers. The revised version of the above referenced manuscript was prepared to address the comments of the Reviewers, as described in detail in the following tables.

To simplify the tracking of the revisions, the added/extended/rewritten parts in the manuscript are listed in response to the Reviewers and all changes are highlighted and/or tracked in the revised manuscript. The numbers denoting sections, subsections, figures, and tables refer to the revised version of the manuscript, unless otherwise noted.

For Peer Review

Comments of Editorial Office	Author's response and revisions
(1) Georisk is a special journal that deals with uncertainties in geotechnical engineering systems and their treatment in engineering risk assessment and management. Please ensure references cited in the manuscript are relevant and up to date. Relevant papers from Georisk should be cited as appropriate to demonstrate the recent progress in the field of georisk.	We recognise the importance of citing relevant and up-to-date literature in Georisk to reflect recent progress in geotechnical risk assessment. We have reviewed the literature and added the following text in the manuscript, along with relevant references from Georisk to appropriately situate our work within the field. Line 250: "…This corresponds to considering the system reliability as a series system, similarly to Daryani and Mohamad (2014)." Line 452: "... It should be noted that the target failure probabilities of retaining walls are still very much unknown (He, Fenton and Griffiths 2022)." Daryani, K. E., and Mohamad, H. (2014). System reliability-based analysis of cantilever retaining walls embedded in granular soils. *Georisk: Assessment and Management of Risk for Engineered Systems and Geohazards*, *8*(3), 192-201. He, P., G. A. Fenton, and D. V. Griffiths (2023). "Calibration of resistance factors for gravity retaining walls." Georisk: Assessment and Management of Risk for Engineered Systems and Geohazards, **17**(3): 586-594.
(2) For revised manuscripts, a clean version is also required to be uploaded for the purpose of production besides the marked version. Please additionally upload the clean version under the category "Supplementary Material - for review".	We will provide the clean version of the manuscript, as recommended.

For Peer Review

(3) Some equations are too long to display correctly, such as Eqs. (18), (19), and many equations in Appendix 2. Please revise those equations in a more appropriate way.	We have revised these equations by reducing the font size of the long equations, allowing them to now appear on a single line for proper formatting and readability. The revised equations are highlighted in yellow.

Comments of Reviewer 1	**Author's response and revisions**
Thank you for submitting your manuscript "Vulnerability Model for Cantilever Retaining Walls Subject to Scour" to Georisk. Your paper addresses an important gap in scour risk assessment for retaining infrastructure. However, several issues must be addressed in the current manuscript:	We thank the Reviewer for highlighting the merits of the study and for their comments, which helped to improve the clarity and quality of the manuscript.
1. Line 22: "simplified approach is then introduced to estimate the scour fragility" - the term switches between "vulnerability" and "fragility" inconsistently throughout the paper. Choose one primary term and use consistently.	We thank the Reviewer for the recommendation. We have used "vulnerability" as the primary term in the revised manuscript.
2. In the introduction section, only limited discussion of existing retaining wall scour research is presented. Only Fael et al. (2006), Khosronejad et al. (2020), and Huang (2017) are cited. A more comprehensive literature review would be great for future readers if possible	Following the Reviewer's advice, we have carried out further search in the literature and identified few additional studies that have now been included in the manuscript (*line 48-71*). "*... Furthermore, scour is frequently overlooked in the design of retaining walls located adjacent to watercourses, a practice that has been associated with catastrophic failures (McKelvey, 2011). Thus, there is a need to develop scour vulnerability and risk assessment procedures accounting for the specific features of these structures.* *The hydraulic processes responsible for scour at the base of longitudinal training walls differ from those acting on bridge piers. A key distinction is that, along retaining walls, lateral flow typically generates elongated scour patterns, whereas pier scour is dominated by downflow and the formation of a horseshoe vortex at the upstream*

For Peer Review

	face. Some studies have examined the hydraulic aspects of the problem, especially the evaluation of the scour depth along walls (Heydari and Diplas 2020). Different approaches have been proposed for estimating the scour depth in longitudinal structures through experimental flume studies and empirical formulations (Fael, Simarro-Grande et al. 2006, Khosronejad, Diplas et al. 2020, Calixto, Castaño et al. 2023, Sotiropoulos and Diplas 2017). It has been found that the development of a scour hole is influenced by a wide range of hydraulic, geotechnical factors and geometry of the problem, including the wall's orientation relative to the approaching flow, local flow velocity and turbulence intensity, sediment transport capacity, and the properties of the riverbed material (Calixto, Castaño et al. 2023, Sotiropoulos and Diplas 2017). Other studies, discussed in Huang (2017), have investigated the failure mechanisms for reinforced retaining walls under toe scouring action, with primary emphasis on coastal settings. However, despite the efforts made on understanding the hydraulic processes and evaluating the scour depth along retaining walls, the influence of scour on the stability of retaining walls has not received sufficient attention. To the best of the author's knowledge, no previous studies have explicitly proposed models to describe the scour vulnerability of these structures" The new references are highlighted in yellow in the reference list.
3. Line 54: "(Theinat et al., 2024)" - this reference is cited but not in the reference list. Please make sure to include all cited studies in the references list.	We apologise for this oversight. The reference has now been added to the reference list, and we have carefully checked the manuscript to ensure that all cited studies are properly included.
4. Line 74-78: "first attempt to develop a closed-form solution" - this is a strong claim. Please include more thorough literature review to justify this statement.	We thank the Reviewer for this valuable comment. While the statement was already qualified with "to the best of the authors' knowledge," we agree that additional context could improve clarity and scholarly rigor. Accordingly, we have expanded the literature review to better position our contribution within existing studies and to substantiate the claim. See response to Comment #2 for additional references identified. The text in the original manuscript:

For Peer Review

	"..this is the first attempt to develop a closed-form solution assessing the scour vulnerability of these structures" has been rewritten as follows in line *70-71*: "..*To the best of our knowledge, no previous studies have explicitly proposed a closed-form solution for assessing the scour vulnerability of these structures*"
5. Line 84: "Plaxis (Plaxis 2020)" - capitalize properly as "PLAXIS" throughout the manuscript for consistency	Thank you for pointing this out. 'Plaxis' has been replaced with 'PLAXIS'
6. Line 96: please include the foundation total width symbol as (B), only Bt and Bh are introduced.	The foundation total width symbol *B* has been included. Text has been rewritten as follows (line 112-113): "*The wall has a total height H, and a foundation width of B, which is made up of the toe length B_t and the heel length B_h.*"
7. Line 108-110, Equation (2): The assumption that scour hole angle equals soil friction angle ϕ' is a major assumption, is this universally acceptable? Doesn't this depend on factors like flow condition, soil type, or rate of scour? Please add more references supporting this assumption or discuss it as a conservative/simplified assumption with potential impacts	Research on how scour holes form next to retaining walls is limited. One flume study used sand with d_{50}=3.5cm, and the scour slopes were close to the effective friction angle of about 40°, similar to the materials drained friction angle φ′ (Sotiropoulos and Diplas 2017). We also add the limitations to this assumption in the manuscript (*line 126-132*): "*This assumption idealizes the scour slope as being controlled only by riverbed material properties. In reality, scour slope angles are also influenced by other factors including wall angles relative to the approach flow, flow velocity and turbulence, sediment transport capacity, and time dependent scour development etc. (Calixto, Castaño et al. 2023, Sotiropoulos and Diplas 2017). The adopted scour angle is therefore intended as a simplified representation for modelling purposes and should be interpreted within the limitations of this assumption.*"
8. Line 147-148: "the effective vertical component of earth pressure forms an angle δ with	The soil–wall interface is actually a soil–soil interface, since the soil above the heel is treated as an integral part

For Peer Review

the effective horizontal component, where δ is assumed equals to soil friction angle ϕ'", dont you think that this is conservative but may be overly so? Typical practice uses δ = (2/3)ϕ' for design. Please discuss this further	of the retaining wall in conventional design practice. We have added the following sentence (*line 170-172*). "*Due to friction at soil-wall interface, the effective vertical component of earth pressure forms an angle δ with the effective horizontal component, where δ is assumed equal to soil friction angle ϕ'. It should be noted that the soil–wall interface is actually a soil–soil interface, since the soil above the heel is treated as an integral part of the retaining wall.*"
9. Line 182: "γ denotes the equivalent soil unit weight" - needs earlier definition. What makes it "equivalent"? Is this saturated unit weight, submerged unit weight, or something else?	The equivalent unit weight is the total weight of the saturated soil below the water level and unsaturated soil above the water level divided by the overall soil volume. Justification has been added in line *206-207*. " $$W_h = B_h \gamma H \quad (24)$$ *where γ denotes the equivalent soil unit weight, which is the total weight of the saturated and unsaturated soil divided by the relevant overall soil volume*"
10. Line 194: "the overturning factor in equation (28) exceeding 1" - but the overturning factor is defined as Mst/Mun, so failure occurs when this is LESS than 1, not exceeding 1. This is contradictory. please make sure to check definition. Typically, factor of safety < 1 indicates failure	Thank you for pointing this out. The text has been revised and now reads as follows (*line 218-219*): "*Overturning failure occurs when the destabilising moments exceeding the stabilising moments, i.e. when the overturning factor defined in equation (28) exceeds 1*" $$f_{ov} = \frac{M_{de}}{M_{st}} \quad (28)$$
11. Line 246: "plain strain state" should be "plane strain state" correct?	Thank you for pointing this out. The typo has been revised.
12. Table 1: RW2 has friction angle of 20° which seems very low for a foundation soil. Is this intentional? Needs discussion	A friction angle of 20° provided only for demonstrating the method and can be replaced with other values. It has been used as an illustrative value representing loose alluvial soils from riverbed material with low strength and bearing capacity. But we agree with the Reviewer that it might be a conservative value, representative of a very low foundation soil.

For Peer Review

	We have clarified this by adding the following sentence (in *line 279-282*): *"It is noteworthy that the value of the friction angle of 20° used for the analysis of RW2 is rather low and has been considered here purely as an illustrative example, representing loose alluvial soils from riverbed material with low strength and bearing capacity."*
13. Table 2: A question please, why is water level ratio (Hw/H) limited to 0.3? Many floods would exceed this. This needs justification or discussion of limitation	We examined the sensitivity of the model output $\gamma_\phi/\gamma_{\phi 0}$ to the wider range of H_w/H. When H_w/H ranges from 0 to 0.3, the total sensitivity index of it is 0.0083. Extending the range to 0-0.5 increases the total sensitivity index only slightly to 0.0149 (see below). The results indicate that H_w/H contributes negligibly to the overall output compared the D_T/D_{Tlim}. 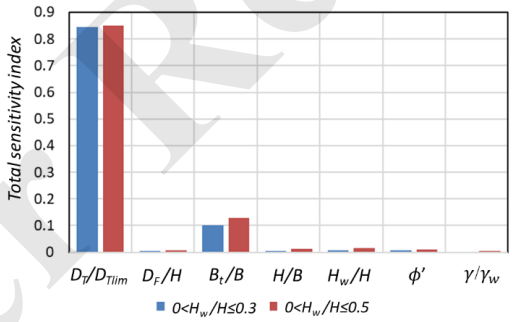 We have added the justification in the text below (*line 343-352*). *"Table 2 illustrates the identified non-dimensional parameters and their range of variation, representing typical retaining wall designs in engineering practice (Sarıbaş and Erbatur 1996, Uray, Çarbaş et al. 2020, Kaveh, Biabani Hamedani et al. 2021). Regarding the water level, $(H_w+D_F)/H$ is assumed to vary between 0 and 0.6, where H_w+D_F represents the portion of the retaining wall below the water level. Accordingly, the relative footing depth D_F/H is assumed to fall within the range 0 to 0.3, and the normalized water depth H_w/H is likewise taken to vary between 0 and 0.3. It should be noted that higher relative water levels than those investigated may occur during extreme events leading to scour. However, considering a wider range of variation for Hw has no impact on the observed results."*

For Peer Review

14. Buckingham, 1914 (cited line 299), appears to be missing in the reference list	The reference has been added. Thank you for highlighting this.
15. - Figures quality needs to be improved, if possible, please make sure all text within figures is readable, like using size 10 Text for example	Thank you for your feedback. We have updated Figure 4, Figure 7, and Figure 9 to improve clarity. Text within the figures has been resized to ensure readability.
Comments of Reviewer 2	**Author's response and revisions**
1.The problem of scour affecting this specific class of structures would benefit from a more detailed introduction. While scour mechanisms and risks are well documented for bridge foundations, retaining walls have received comparatively less attention in the literature. Providing additional context, explanations, and real-world examples of failures or damage would help underline the significance and relevance of the study	We thank the Reviewer for highlighting the merits of the study. Scour-induced retaining wall failures have been reported in the UK, including for example a garden wall collapse into the River Tawe in Powys following prolonged undercutting and sinkhole formation (County Times, 2024), and a retaining wall failure in Sheffield that led to significant property damage and emergency response (BBC News, 2024). 1) County Times (2024). *Family's garden wall collapses into River Tawe in Powys*. [Online] Available at: https://www.countytimes.co.uk/news/24097484.familys-garden-wall-collapses-river-tawe-powys/ 2) BBC News (2024). *Sheffield retaining wall collapse prompts emergency response*. [Online] Available at: https://www.bbc.co.uk/news/articles/cly4ym121xjo It is noteworthy that the research underpinning this paper was funded by National Highways, the largest transport infrastructure agency in the UK. National Highways is responsible for the risk assessment and management of numerous retaining walls and commissioned this study because formal procedures for undertaking this task are not yet in place. We have carried out a further search in the literature and identified few additional studies that have now been included in the manuscript (*line 48-71*). *"Furthermore, scour is frequently overlooked in the design of retaining walls located adjacent to*

For Peer Review

	watercourses, a practice that has been associated with catastrophic failures (McKelvey, 2011). Thus, there is a need to develop scour vulnerability and risk assessment procedures accounting for the specific features of these structures. *The hydraulic processes responsible for scour at the base of longitudinal training walls differ from those acting on bridge piers. A key distinction is that, along retaining walls, lateral flow typically generates elongated scour patterns, whereas pier scour is dominated by downflow and the formation of a horseshoe vortex at the upstream face. Some studies have examined the hydraulic aspects of the problem, especially the evaluation of the scour depth along walls (Heydari and Diplas 2020). Different approaches have been proposed for estimating the scour depth in longitudinal structures through experimental flume studies and empirical formulations (Fael, Simarro-Grande et al. 2006, Khosronejad, Diplas et al. 2020, Calixto, Castaño et al. 2023, Sotiropoulos and Diplas 2017). It has been found that the development of a scour hole is influenced by a wide range of hydraulic, geotechnical factors and geometry of the problem, including the wall's orientation relative to the approaching flow, local flow velocity and turbulence intensity, sediment transport capacity, and the properties of the riverbed material (Calixto, Castaño et al. 2023, Sotiropoulos and Diplas 2017). Other studies, discussed in Huang (2017), have investigated the failure mechanisms for reinforced retaining walls under toe scouring action, with primary emphasis on coastal settings. However, despite the efforts made on understanding the hydraulic processes and evaluating the scour depth along retaining walls, the influence of scour on the stability of retaining walls has not received sufficient attention. To the best of the author's knowledge, no previous studies have explicitly proposed models to describe the scour vulnerability of these structures"*
2. Equation (1) assumes that during the first stage $DT \leq DF$, which seems to imply that the term remains strictly positive. If this is not always the case, a clarification is needed	The effective foundation depth is always either positive or zero ($D'_F \geq 0$). This is expressed in equation 1: $$D'_F = \max(0, D_F - D_T)$$
3. In Section 5, the safety factor is evaluated through a numerical	Thank you for pointing this out. We have added additional numerical staged-construction steps in

For Peer Review

model. However, the description of how the model operates is somewhat limited. Providing additional details on the procedure.	PLAXIS, following the model description and the adopted parameters (*line 287-293*). "*Each case study was analysed in PLAXIS using a three-stage construction procedure. In the first stage, the retaining wall and the initial ground conditions were activated and brought to equilibrium. In the second stage, the scour process was simulated by progressively removing soil elements around the wall until a new equilibrium state was achieved. In the final stage, a strength-reduction analysis was performed, in which the shear strength parameters ϕ' and c were systematically reduced to identify the onset of global failure of the retaining wall system*"
4. It is not entirely clear how Equation (32) was obtained. Was it derived analytically, or fitted through regression or another approximation method?	Equation (32) is fitted through regression.
5. The notation used in line 370 appears inconsistent with that shown in Figure 9. For example, some gamma symbols are written with capital letters in the text but not in the figure. Please check.	Thank you for highlighting this. The symbols have been updated and are now consistent.

For Peer Review